2012-07-13

Analog Feedback Control of Broadband Fan Noise

Cole Victor Duke
Brigham Young University - Provo

Analog Feedback Control of Broadband Fan Noise

Cole V. Duke

A thesis submitted to the faculty of
Brigham Young University
in partial fulfillment of the requirements for the degree of

Master of Science

Scott D. Sommerfeldt, Chair
Kent L. Gee
Jonathan D. Blotter

Department of Physics and Astronomy

Brigham Young University

August 2012

ABSTRACT

Analog Feedback Control of Broadband Fan Noise

Cole V. Duke
Department of Physics and Astronomy, BYU
Master of Science

Active noise control (ANC) has been implemented using analog filters to reduce broadband noise from a small axial cooling fan. Previous work successfully attenuated narrow-band, tonal portions of the noise using a digital controller. The practical performance limits of this system were reached and it was desirable to attenuate the noise further. Additional research, therefore, sought to attenuate broadband noise from the fan using a digital controller, but performance was limited by the group delay inherent in the digital signal processor (DSP). Current research attempts to further attenuate broadband noise and improve performance of the system by combining the tonal controller with an analog feedback controller. An analog controller is implemented in parallel with the digital controller without degrading the performance of either individual controller. Broadband noise is attenuated in a certain frequency region, but at the expense of increasing noise in adjacent frequency regions. Results show that a single-input single-output (SISO) controller is preferable to a multiple-input multiple-output (MIMO) controller for this system.

Keywords: active noise control, fan noise, feedback control, analog filters

ACKNOWLEDGMENTS

I want to express my sincere gratitude to the following individuals. Without them, this work would not have been possible.

- Scott Sommerfeldt, my advisor, for taking the time to share his knowledge and experience with me, for continually teaching and counseling me, and for sticking with me throughout the research and writing process
- Kent Gee and Jon Blotter for teaching and guiding me
- Brian Monson, Matt Green, Connor Duke, and Ben Shafer for paving the way for fan noise research at BYU
- The BYU Acoustics Research Group for their passion for acoustics
- Lacey, Alex, and Jonny for their love and support, and for making this all worth it
- Mom and Dad for their endless help and encouragement throughout the writing process

Contents

List of Figures

Chapter 1

Introduction

1.1 Active noise control

Active noise control (ANC) is the process of reducing the amplitude of an acoustic field by introducing a secondary acoustic field. This is accomplished through destructive wave interference. That is, the noise from an existing noise source, or primary source, can be attenuated by introducing an acoustic signal from a secondary source. The outcome is dependent upon many factors, including relative magnitude and phase of the two sources, physical construction, and orientation of the primary sources, the secondary sources, and the error sensors.

The concept of ANC was first described in a patent by Paul Lueg [1,2]. While his experimental attempts only had limited success, the principle survives. It involves using a microphone to sense a primary noise signal, electronically manipulating it, and sending it through a secondary acoustic source. This foundation is what successive ANC refinements are based on today. In addition, early work in ANC was implemented through analog filters. However, due to the drifting properties of electronic components, performance was typically limited by instability, causing the controller to amplify the disturbance rather than attenuating it. Due to its relative simplicity, most early attempts

at ANC involved one-dimensional sound fields in ducts or enclosures.

With the advent of computers and digital signal processors (DSP) in recent years, ANC has become practical for many applications beyond the one-dimensional scope of initial experiments. Digital systems offer obvious advantages over analog controllers. A digital controller can be designed to track the output from the system and adapt the control filter to account for changes in the disturbance signal, or even changes in the physical system. This adaptability can prevent a system from becoming unstable when changes do occur. However, digital systems also have more inherent delay than analog controllers, which can render them less effective for some applications.

Continued research has also studied the fundamentals of ANC in more detail. This has led to systems that are more physically viable and robust, while also performing better. For example, it has been discovered that, through the principle of mutual source coupling, a compact system with all transducers placed closely to the primary source can be used to attenuate noise globally in three dimensions.

1.2 Fan noise

As electronic devices, such as computers and projectors, become more prevalent in everyday environments, the noise they produce contributes more to the overall disturbance level in homes and offices. For example, as electronics become faster, smaller, and more complex, they generally produce more heat. In turn, they require more cooling, which is typically achieved through small internal cooling fans.

Noise from fans can be described as the superposition of two different types of noise. As illustrated in Figure 1.1, the tonal noise typically dominates the spectrum, with the broadband noise at a lower and more consistent level between the tonal peaks. The tonal peaks are generally created by the periodic passage of the fan blades as the fan spins, while broadband noise is created

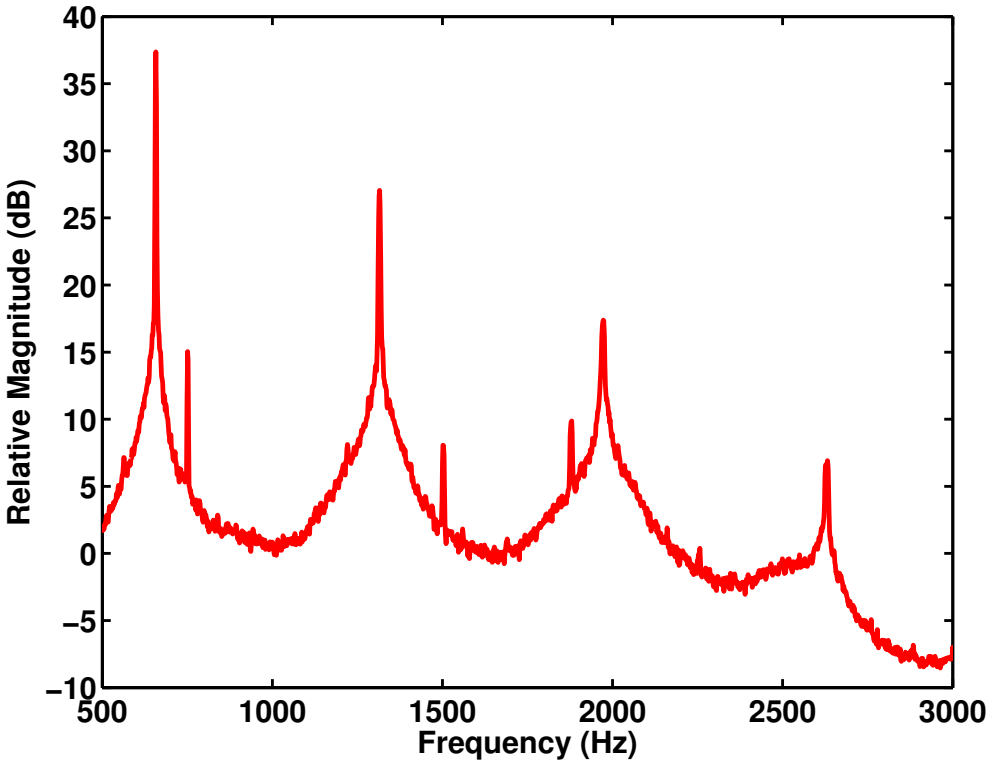

Figure 1.1 A typical fan noise spectrum containing broadband and tonal components.

by many processes. These include turbulence around the rotor and at the trailing edge of the fan blades, as well as leakage around the blade tips [3] .

1.3 Past work in fan ANC

Significant research has been performed in the active control of tonal fan noise. It has been successfully shown that tonal fan noise can generally be attenuated down to the level of the broadband noise using a digital controller, as shown in Figure 1.2, which shows result at the error sensor when active control is applied to the current system under study. It has also been shown that the limit of achievable control of tonal noise has not yet been reached [4, 5]. For this reason, it makes sense that the next step would be to attenuate the broadband noise if improved overall attenuation is to

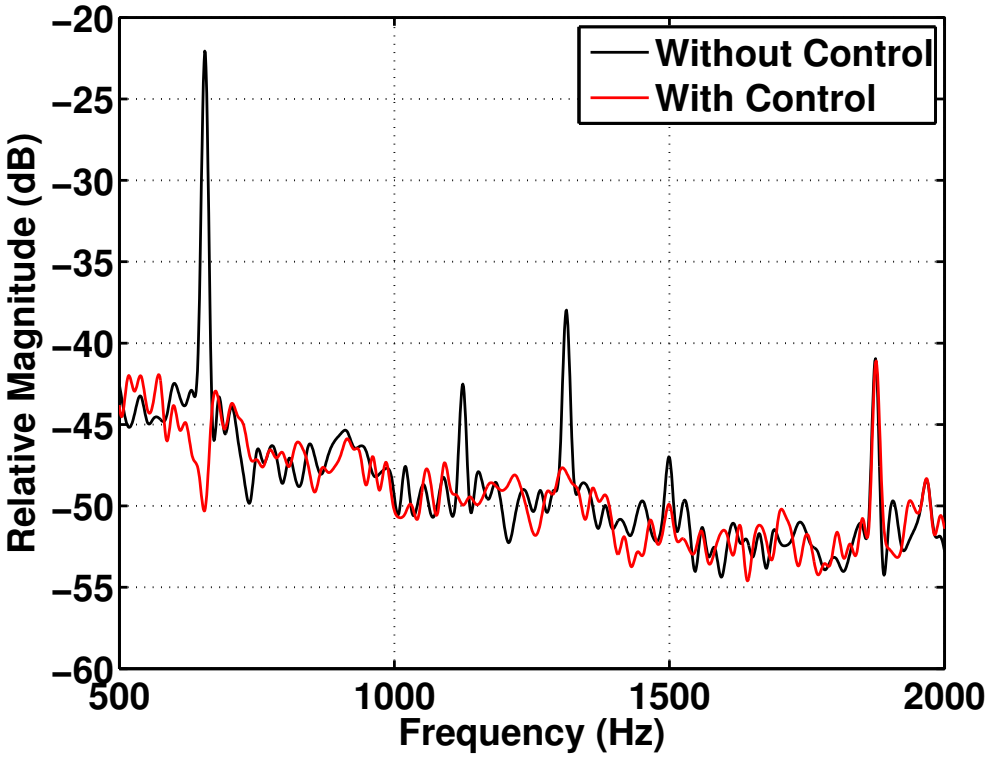

Figure 1.2 An example of tonal control of fan noise at the error sensor.

be achieved. Some research has been conducted to attempt to attenuate broadband noise, with its success primarily realized in the digital domain. However, the delay inherent in the DSP has limited the success achieved in broadband noise attenuation [6].

Meanwhile, previous research has shown that noise can be attenuated in the far field using only near-field sensors and actuators. The proper placement of near-field actuators results in a phenomenon known as mutual source coupling. Source coupling occurs when acoustic sources are brought close to one another, relative to a wavelength, and the radiation impedance seen by each source is modified by the radiation of the other source. The secondary source strength can therefore be adjusted to decrease radiation impedance on the primary source and therefore reduce global radiation. However, if it is desired to also bring the error sensors into the near field, previous research has shown that the sensors must be placed in specific locations if global attenuation is to be

achieved [4,7]. This coupling makes control systems more feasible because it can be self-contained in a small space without the need for far-field error sensors. However, it imposes restrictions on the performance of the feedback controller. This limitation will be discussed in Section 3.3.

1.4 Research overview

The existing ANC system performs well, and has been studied and optimized within its constraints. It is effective at reducing the tonal noise components in fan noise down to the general level of the broadband noise. All transducers are located close to the fan, so the system could be implemented in most desktop computers without increasing the size of the computer. The system attenuates noise in three dimensions, and the reduction is nearly uniform in all directions, which further adds to the feasibility of the system. It can also track changes in fan speed. As shown in Figure 1.3, the system's setup consists of a small cooling fan mounted in a mock computer case. The fan is closely surrounded by four symmetrically-placed loudspeakers which act as control actuators. Four electret microphones, which act as error sensors, are also placed near the fan. The goal of the control system is to reduce sound pressure at the error sensors, which has been shown to directly lead to a reduction in global sound power, assuming proper placement of the error sensors.

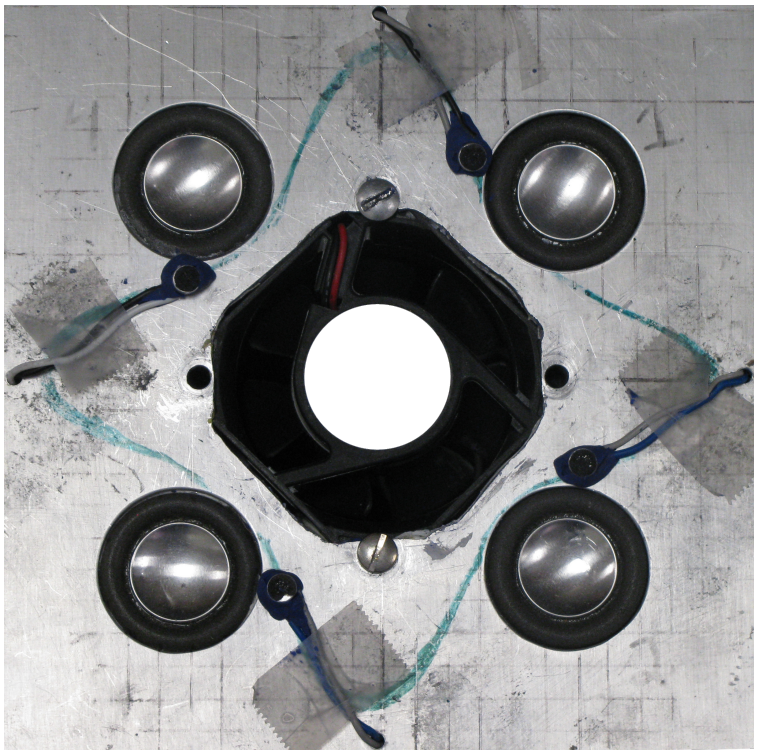

Figure 1.3 Fan with control loudspeakers and error-sensing microphones

The goal of the current research is to augment the performance of the existing ANC system by implementing a controller that will serve to attenuate the portion of the broadband noise that is unaffected by the tonal controller. In the current system, the tonal portion of the fan noise is controlled using a digital controller. For reasons which will be discussed in Chapter 2, this type of controller is not feasible to control the broadband noise. Therefore, an analog feedback controller will be used in conjunction with the existing digital controller to attenuate the tonal and broadband portions of the fan noise.

This is accomplished using a combination of well-known filter types. A computer model of the system has been developed, in which the control filter parameters can be adjusted and the performance predicted. Multiple types of control filters are studied in a single-channel configuration. One particular filter is judged as performing well, and is then implemented in a multiple channel

configuration. The multiple channel configuration is combined with the existing tonal noise controller to measure overall performance, and to evaluate any negative effects the two systems may have on one another.

1.5 Thesis Organization

Chapter 2 explores in greater depth the concept of ANC, and specifically its application to fan noise. Chapter 3 consists of a detailed overview of the concept and limitations of feedback control. Chapter 4 contains background on the use of analog filters as well as many common types and implementations, or topologies, of filters. Chapter 5 contains an overview of the physical system as well as the filters that were used throughout the research process. Chapter 6 contains experimental results and analysis. Chapter 7 discusses conclusions based on these results as well as suggestions for future work.

Chapter 2

Active Control of Fan Noise

2.1 Digital control for tonal noise

Previous research has shown that a digital controller can be used to attenuate tonal noise from a fan [3, 4]. This has been implemented using a digital controller in a feed-forward configuration. A block diagram of this system is illustrated in Figure 2.1. The use of variables n and z denote a discrete-time domain. The variable n represents discrete time, or sample, and z represents discrete frequency calculated using a Z-transform [8]. The blocks in the diagram represent discrete transfer functions of the system and controller. Here, *d(n)* represents the disturbance signal to be controlled, which is the fan noise in the case of this research. Also, *x(n)* represents a reference signal, or a signal that is correlated with the disturbance signal. The plant, P(z), represents the physical system that is generating noise, as well as the acoustic path to the error sensor. W(z) represents the control filter. H(z) represents the secondary noise path, which is the path from the controller through the control loudspeaker and out to the error sensor. $\hat{H}$(z) represents an approximation of the secondary control path. The error signal, *e(n)*, is then used to calculate updated coefficients for the control filter. This algorithm is referred to as a Filtered-X LMS algorithm [9]. The filtered-x refers to the

fact that there is a filtered reference input to the LMS update operation, and LMS refers to the fact that the controller is updating so as to minimize the mean squared error (least mean square). The updating of the control filter not only serves to minimize the squared error of the system, but it can also reflect any changes in the system, such as the plant, the secondary path, or even the disturbance signal itself. The Filtered-X LMS algorithm can rapidly track changes in the disturbance signal, is robust to errors in the estimation of the secondary path, and is relatively easy to implement [9, 10].

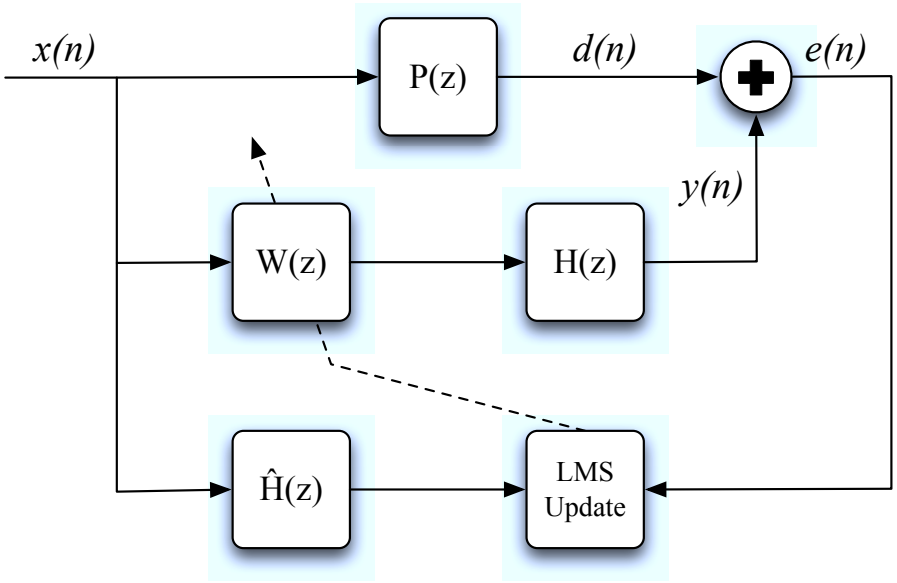

Figure 2.1 Block diagram of the Filtered-X LMS system.

This type of controller has shown successful performance due to specific characteristics of tonal fan noise [6]. First, since such noise can be tied directly to the rotational speed of the fan, a tachometer signal can be used as a reference signal for the controller. Second, tonal noise is periodic. Research has shown that maximum attenuation is limited by the autocorrelation of the disturbance signal [11]. But, since a tonal signal is periodic, its autocorrelation is periodic as well. Therefore, group delay in the system will not affect control performance because the signal will be correlated with itself periodically. Finally, the system is adaptive and can therefore track changes

in fan speed and allow for adjustment of the control filter accordingly.

Previous work has also demonstrated significant tonal noise attenuation using an adaptive digital controller in a feedback configuration [12]. This can be useful in a situation where the disturbance signal has dominant tonal components, but there is no feasible reference signal to use as input to the controller. Therefore, the nature of tonal noise will overcome the limits of delay in digital systems.

2.2 Global reduction

The system being researched consists of control actuators and error sensors, all in close proximity to the fan. However, the goal of the noise control system is to reduce the global radiation far from the fan. This can be achieved through a principle known as mutual source coupling, as discussed in Section 1.3. The ability to produce source coupling between the fan and the loudspeakers is heavily dependent on the location of the control actuators.

The global radiation of the fan coupled with the loudspeakers can be analytically minimized. Figure 2.2 shows a map of the sound pressure in the near field when the far-field sound power is minimized. The color bar shows pressure in dB, referenced to an arbitrarily chosen P_0. The circle in the middle represents the fan, and the stars represent the control loudspeakers. The dark blue region corresponds to a minimum in pressure. It has been shown that if error sensors are placed on this nodal line, then the controller will force the near-field pressure to match the theoretical minimum quite well, and will therefore produce significant attenuation of global sound power [5, 13].

However, this restriction on error sensor placement imposes a necessary amount of delay into the system. Since the acoustic path between a control loudspeaker and a corresponding microphone is part of the system to be controlled, the delay associated with this acoustic path must be accounted for by the controller. The error sensors will be placed as close to the control loudspeakers as

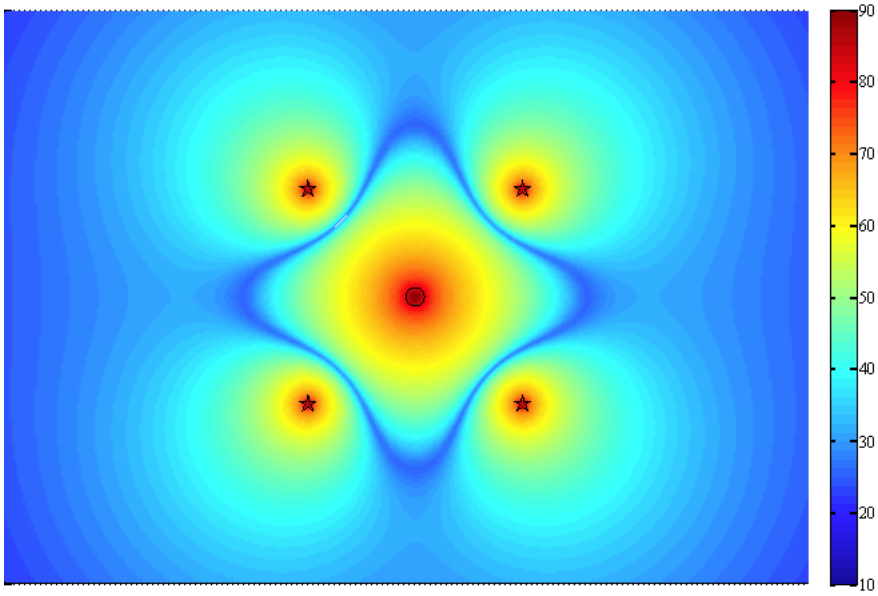

Figure 2.2 Near-field sound pressure (dB) when far-field sound power is minimized.

possible while still adhering to the limitations which provide global reduction.

2.3 Digital control for broadband noise

Feed-forward control is not effective in controlling broadband noise from a fan because there is no feasible way of obtaining a reference signal. There is no physical structure, such as fan blades rotating, that can be correlated to the disturbance. For this reason, a feedback controller is necessary.

Previous research involved using a digital feedback controller for broadband fan noise. It was demonstrated that attenuation is theoretically limited because of the delay associated with the feedback loop, a significant portion of which is the inherent delay associated with the DSP. The maximum achievable attenuation of a signal, through feedback control, is given by

$$Attenuation_{dB}(t) = -10 * log(1 - \frac{E_p(t)}{E_{total}}). \tag{2.1}$$

E_{total} is the autocorrelation of the disturbance signal at time 0, which is defined to be 1 in a nor-

malized autocorrelation. $E_p(t)$ represents the maximum of the autocorrelation of the disturbance signal at time greater than t [6, 9]. This equation results in a monotonically non-increasing value for maximum attenuation with increased group delay. Therefore, the value of maximum attenuation will never increase with increased group delay. The value will be constant if the maximum autocorrelation occurs at time greater than t.

Noise from the current fan under test was measured at the error sensor, and this noise was used to calculate possible attenuation versus group delay. Based on this calculation, the maximum theoretical attenuation of the fan noise with relation to group delay is shown in Figure 2.3. The digital control system studied had a total of 650 μs of delay. It was approximated that 368 μs of this was introduced by the DSP and its associated hardware, including anti-alias filters and reconstruction filters. The current fan system would predict approximately 1.6 dB of theoretical attenuation for this much delay. It was ultimately determined that this amount of delay theoretically limited the maximum possible attenuation to the point where control was not significant. [6].

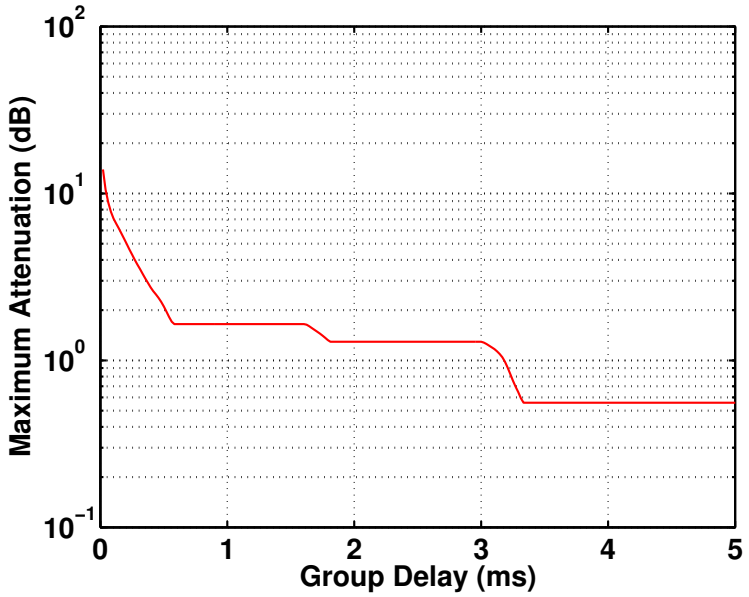

Figure 2.3 A plot of the maximum theoretical attenuation vs. total group delay.

2.4 Analog control for broadband noise

The current research investigates the use of analog control for broadband fan noise. Analog noise control consists of an analog filter which is designed to provide noise attenuation in some control band when combined with the plant. The amount of attenuation achievable is dependent on the magnitude and phase of the open-loop system when the filter is implemented. An analog controller will introduce far less delay, and therefore phase, than a digital controller, and it may therefore be possible to attenuate the noise more than was possible with a digital controller. However, a simple analog controller has limitations as well, such as not being able to adapt to changes in the control system.

The remainder of this thesis will focus on the use of analog feedback control to reduce broadband fan noise, and will discuss the performance and limitations of such a controller.

Chapter 3

Feedback Control

3.1 Definition of feedback control

Feedback occurs when the output of a system directly affects, or contributes to, the input of the system. Feedback control is the process of manipulating a system's output and then combining it with the input to achieve a desired final output from the system [14]. A block diagram representing the current hardware can be seen in Figure 3.1. W(ω) represents the controller, which could be either a DSP or an analog filter. P(ω) , known as the plant, represents the rest of the system to be controlled. In the current research, this represents the electrical/acoustical path from the output of the controller, which drives the loudspeaker, to the input of the controller, which comes from the microphone. The signal, d(t), represents the fan noise received at the error sensor. The noise is then passed through the control filter and back through the plant. The purpose of the controller is to attenuate noise at the error sensor. The junction where y(t) and d(t) combine can be thought of as the error sensor. This is the location where the disturbance signal will be sensed, as well as the location where control will be achieved.

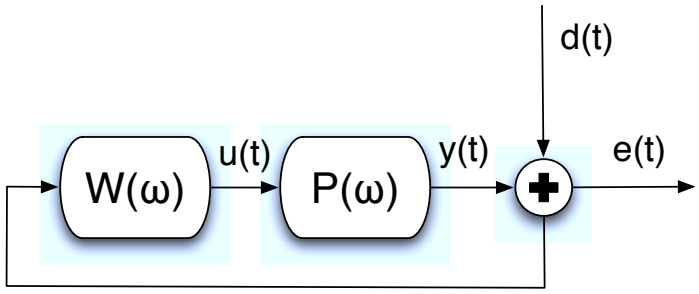

Figure 3.1 A block diagram of the current feedback system.

3.2 Stability

The system shown in Figure 3.2 represents an open-loop system. This is simply the plant in series with the control filter. Typically, feedback control design is done on the open loop system. There are criteria that the open loop system must meet in order to ensure a stable output when implemented as a closed-loop system.

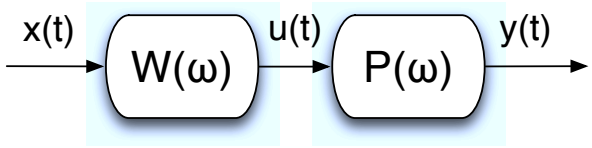

Figure 3.2 Open-loop feedback system.

The stability of a system that incorporates feedback is dictated by the Nyquist Stability Criterion, which states that the phase of the open loop system response must be less than -180 degrees at unity gain (0 dB) [15]. However, this is a simple criterion that does not account for systems with significant delay. It is also specific to cases where the magnitude response of the plant decreases with increased frequency. These requirements are typically met for mechanical systems where feedback control is used to control the time response of the system. However, many acoustical systems do not meet these criteria. In cases such as these, stability must be considered as a function

of frequency. That is, stability must be separately evaluated at different frequency bands.

For this study, the design of the feedback controller was done in the frequency domain. When considering ANC systems in the frequency domain, the system can be viewed in terms of wave superposition. When two acoustic waves combine, the magnitude of the resulting wave depends on the relative phase of the two initial waves. Figure 3.3 illustrates that when two waves have the same phase at a given frequency, their magnitude will increase, resulting in constructive interference. When two waves are out of phase by -180 degrees, and their magnitudes are equal, they will completely cancel out one another through destructive interference. However, between these two extremes, there is a continuum of relative phases possible for two waves interfering with one another.

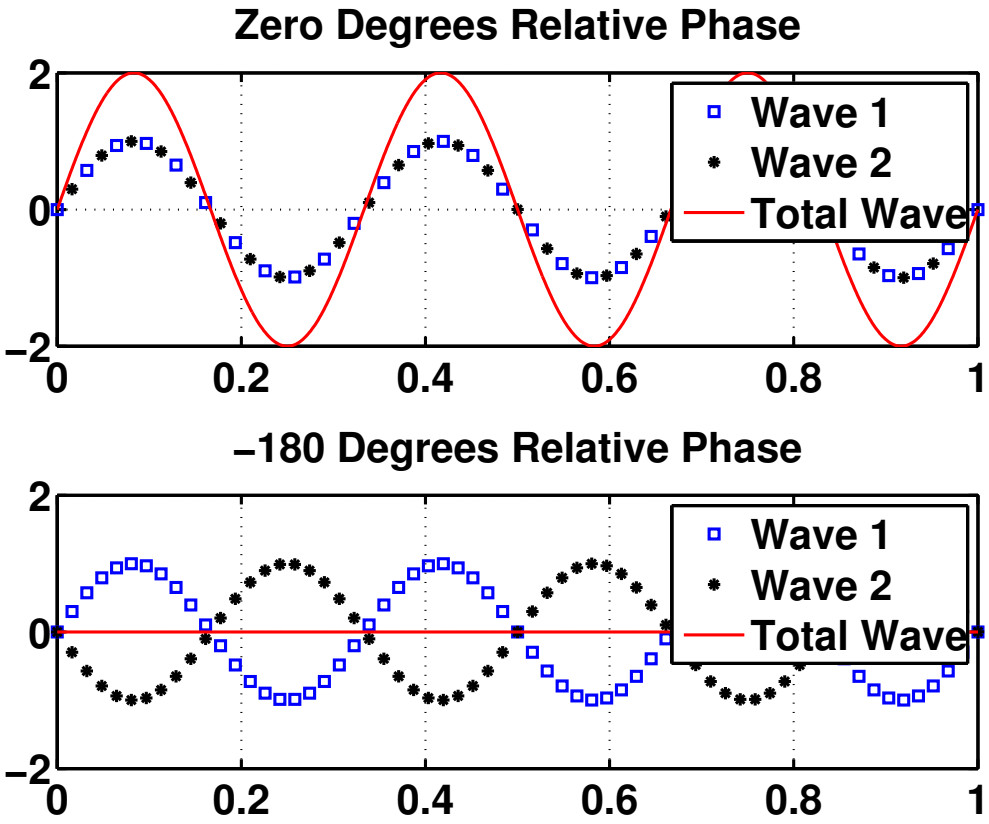

Figure 3.3 Result of wave superposition in and out of phase

Figure 3.4 shows how waves can interfere with varying relative phases. If two sine waves of the same frequency and magnitude but with varying relative phase interfere, the resultant wave will have the magnitude indicated in the figure. As expected, there is complete cancellation at -180 degrees of relative phase, and a doubling of magnitude at 0 degrees of relative phase. It is interesting to note where the crossover points occur between constructive and destructive interference, where the combined resultant wave has the same magnitude as the original waves.

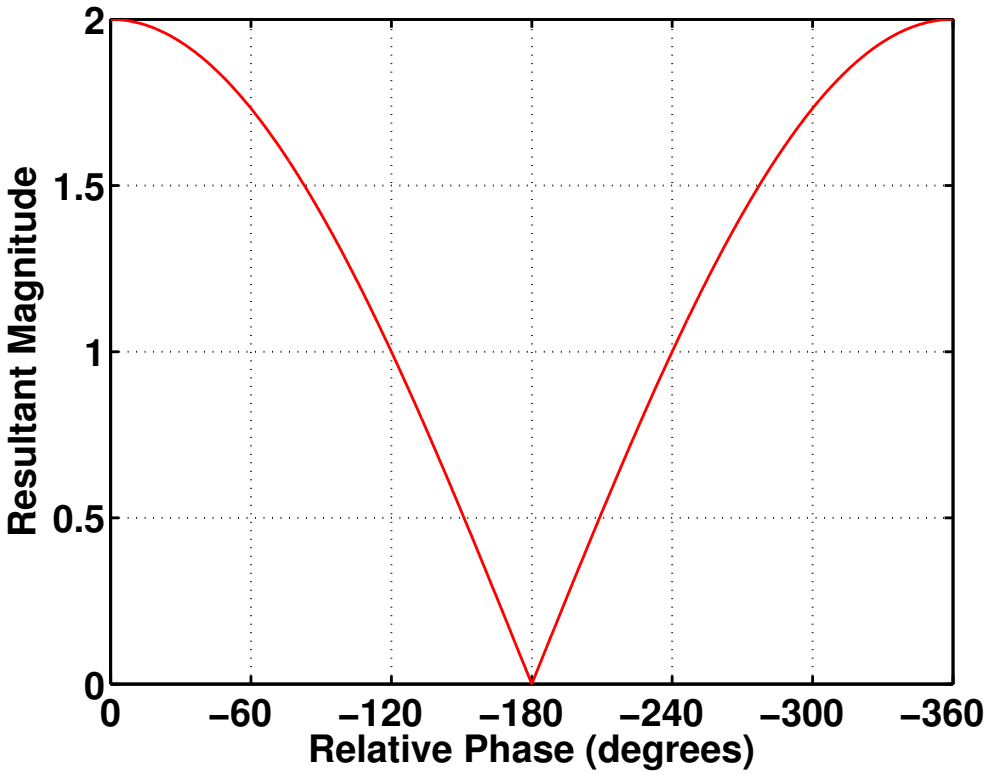

Figure 3.4 Result of wave superposition with varying relative phase

This illustrates that there is a range of phase, between -120 and -240 degrees, that will result in destructive interference and attenuation. Any phase outside of this range will result in constructive interference, creating a combined wave with larger amplitude than the original. Therefore, designing an effective, stable system is dependent on increasing the destructive interference while simultaneously decreasing the constructive interference. The feedback controller should therefore

be designed so that the open loop response has greater than unity gain in regions of phase between -120 and -240 degrees, and decreased gain outside of this region.

3.3 Group delay

Since the performance of the feedback controller is dependent on the magnitude and phase of the entire open loop system, we must first consider the magnitude and phase of the plant. The magnitude of the plant is primarily shaped by the response of the control loudspeaker, while the phase of the plant is dominated by the acoustic delay between the loudspeaker and the error sensor. Figure 3.5 shows how this delay affects the possible control region. Without any type of filtering, the possible control region between -120 and -240 degrees of phase is already limited to between 300 Hz and 2000 Hz. Meanwhile, the areas with the highest magnitude response are outside of this region. This demonstrates the need for some type of filtering to avoid noise amplification and possible instability.

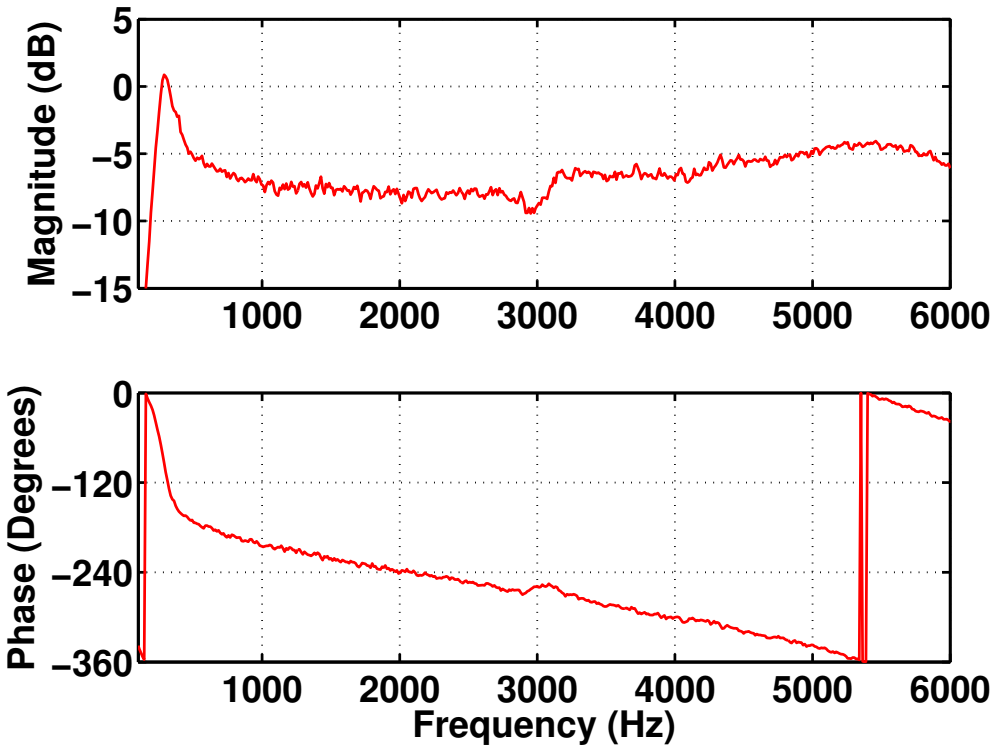

Figure 3.5 Magnitude and phase response of the plant.

3.4 Waterbed effect

Bode's integral formula, expressed as

$$\int_0^\infty log|S(i\omega)|d\omega = \int_0^\infty log\frac{1}{|1+L(i\omega)|}d\omega = \pi\sum p_k, \tag{3.1}$$

illustrates that there are fundamental limitations to what can be achieved with feedback control. In this equation, $i\omega$ represents frequency, and $L(i\omega)$ represents the transfer function of the open-loop system across frequency.

$$\frac{1}{1+L(i\omega)} \tag{3.2}$$

is commonly referred to as the sensitivity function, and is written $S(i\omega)$. At frequencies where $|S(i\omega)| < 1$, feedback will cause the disturbance to be attenuated. At frequencies where $|S(i\omega)| >$

1, feedback will cause the disturbance signal to be amplified [16].

When integrated across frequency, $log|S(i\omega)|$ can be simplified to a summation of all of the unstable poles of the transfer function, or all of the poles in the right-half of the frequency plane (p_k). In an unconditionally stable system, there are no poles in the right-half plane, and this sum will therefore be zero. However, even in conditionally stable systems or unstable systems, there are a finite number of unstable poles, and therefore the integral of the sensitivity function is constant. Therefore, if the controller acts to decrease sensitivity at one frequency, resulting in disturbance attenuation, it must be offset by increased sensitivity at another frequency, resulting in disturbance amplification. Since the disturbance reduction in one frequency band will effectively amplify the disturbance in adjacent frequency bands, this phenomenon is typically referred to as the waterbed effect. Figure 3.6 is a representation of the waterbed effect. When the disturbance signal is attenuated, signified by the blue arrow, it is necessarily amplified in the adjacent frequency regions, signified by the red arrows. This implies that feedback noise control should be designed to target frequencies where the disturbance signal is greatest, and where the resultant disturbance amplification at other frequencies will be less noticeable.

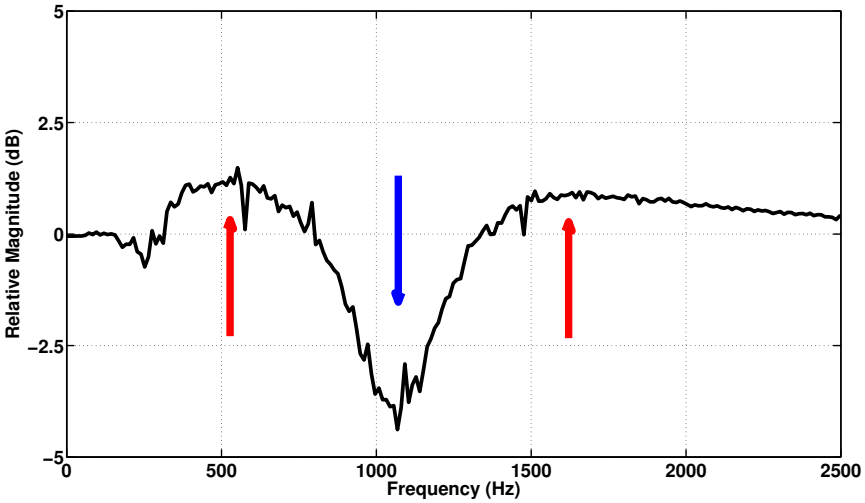

Figure 3.6 Graphical representation of the waterbed effect.

3.5 MIMO vs. SISO control

For systems with multiple inputs and multiple outputs, a controller can be designed in one of two ways. A single-input and single-output (SISO) controller, also known as a decentralized controller, involves multiple controllers acting independently. This type of controller is typically designed to control only the inputs and outputs with the strongest interaction. This control configuration is simpler to design and implement, and can be relatively stable. However, it does not account for every interaction between inputs and outputs, which can possibly hinder performance or cause instability.

Multiple-input multiple-output (MIMO) control, or centralized control, involves the design of a controller which accounts for each input and output of the system and each interaction between them. In a system with M inputs and N outputs, this type of control must account for MxN plants [17]. A MIMO controller is more complex, but it can be more effective, and may be required in specific applications where the secondary interactions are significant. Put another way, the need for MIMO control depends on the amount of mutual interaction between inputs and outputs.

For the purposes of the current research, the error sensor is considered to be the input to the controller. The output of the plant can be considered as the output from the loudspeaker, including the propagation back to the error sensor. For simplification in discussing MIMO control, we will simply consider the plant to be the propagation path from the loudspeaker to the microphone. Figure 3.7 illustrates how this relates to a single channel of the control system. One loudspeaker and the nearest microphone can be considered a SISO control system. For the system under test, SISO control can be designed independently for each of the four speaker/microphone combinations. This type of controller is depicted in Figure 3.8

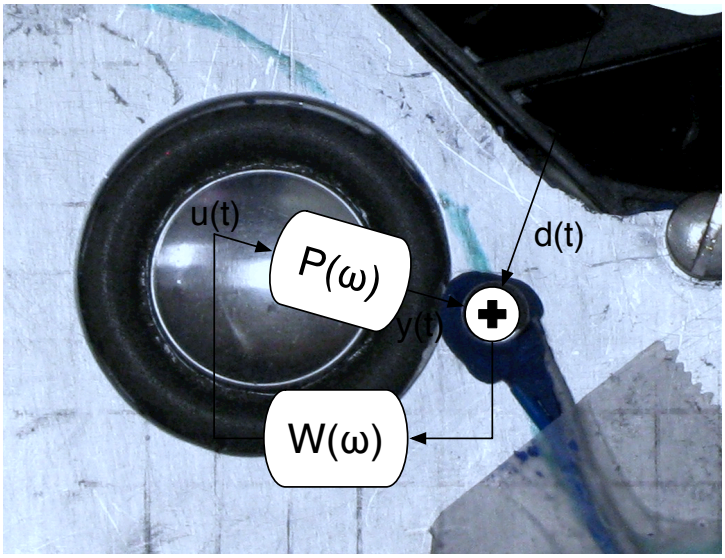

Figure 3.7 Photo of single-channel control system with block diagram overlay.

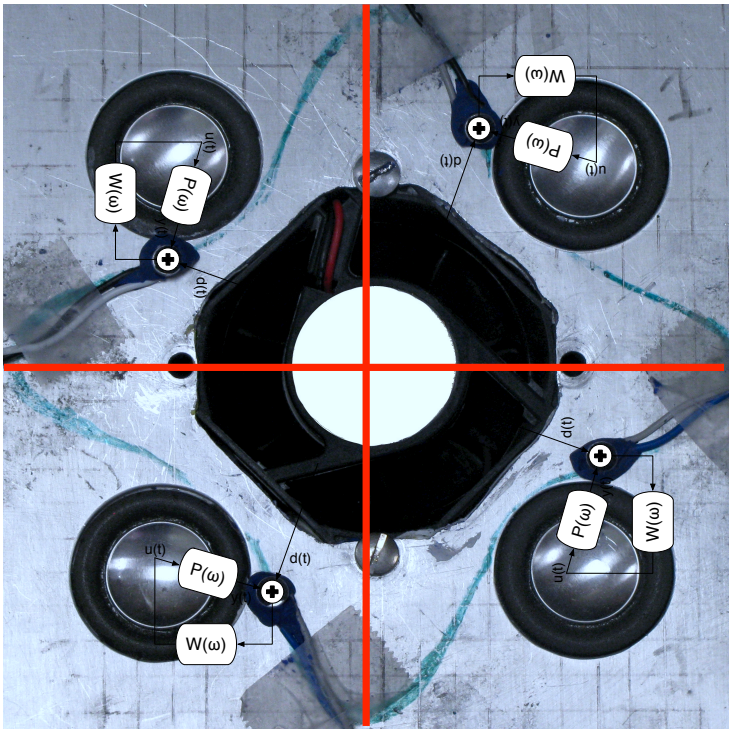

Figure 3.8 A photo of the complete SISO system with block digram overlay.

However, the current configuration consists of four loudspeakers and four microphones, all of which interact in the physical domain. This complicates the control problem because each loudspeaker/microphone combination is not an independent control system. The output from any single loudspeaker will propagate to each of the four microphones. Since each of the four speakers will interact with each of the microphones, this MIMO system consists of sixteen plants. Take u_m to be the m^{th} input to the system, or the signal to the m^{th} loudspeaker. Take y_n to be the n^{th} output, or the n^{th} error microphone signal. Then p_{nm} represents the time-domain impulse response of the plant, consisting of the response of the m^{th} loudspeaker, the acoustic propagation to the n^{th} microphone, and the response of the n^{th} microphone. The input-output equation of the system can therefore be written as

$$\begin{bmatrix} y_1 \\ y_2 \\ y_3 \\ y_4 \end{bmatrix} = \begin{bmatrix} p_{11} & p_{12} & p_{13} & p_{14} \\ p_{21} & p_{22} & p_{23} & p_{24} \\ p_{31} & p_{32} & p_{33} & p_{34} \\ p_{41} & p_{42} & p_{43} & p_{44} \end{bmatrix} \otimes \begin{bmatrix} u_1 \\ u_2 \\ u_3 \\ u_4 \end{bmatrix}, \tag{3.3}$$

where $\otimes$ represents time-domain convolution.

The p-matrix in this equation is referred to as the relative gain matrix(RGM) [18, 19]. This matrix can be used to evaluate the mutual interaction between each input and output combination. In the current system, the case where m=n represents the m^{th} loudspeaker and the closest microphone. Therefore, the diagonal elements of the RGM have the largest magnitude, representing the strongest interaction. Comparing the magnitude of the off-diagonal elements to the diagonal elements can reveal whether or not a MIMO type controller is necessary to ensure optimal control. If the magnitude of the off-diagonal elements is insignificant relative to the diagonal elements, then a SISO controller may be sufficient.

Chapter 4

Analog Filters

4.1 Chapter Overview

For successful feedback control implementation, it is necessary to find an appropriate control filter to affect noise attenuation when the feedback loop is closed. This section outlines a number of well-known filter types and topologies, and their viability as control filters in the current system is investigated in Chapter 5.

Filter type describes the magnitude and phase response of the filter based on certain variables, such as cutoff frequency and ripple width. Filter topology describes the physical implementation of the filter, including physical components (resistors, capacitors, operational amplifiers) and their configuration. The values of these components then dictates the filter characteristics.

As discussed in Section 3.2, the magnitude and phase of the plant must be modified before feedback control can be successfully applied. If this is not done, either the disturbance will be amplified, or the system will be unstable. The objective is to modify the response of the system in such a way as to maximize gain in regions of frequency that will result in attenuation (-120 to -240 degrees), while limiting the gain at other frequencies, thereby limiting disturbance amplification.

This is done using analog filters.

However, utilizing filters for stability will also necessarily introduce more delay into the system. Therefore, the goal is to apply enough filtering to shape the magnitude response of the open-loop system without introducing so much delay that the region of control is unduly limited.

4.2 Filter Topologies

4.2.1 Sallen-Key

In 1955, Sallen and Key proposed a novel way of designing filters with complex poles [20]. This was done using resistors, capacitors, and vacuum tubes. Soon after, as integrated circuits became popular, Sallen-Key filters were then designed using operational amplifiers, or op-amps [21]. This type of filter is popular because of its simplicity, due to the fact that it requires only one op-amp to implement a second-order filter. However, its performance is heavily dependent on the bandwidth of the op-amp used [22]. At acoustic frequencies, however, this is typically not an issue. A schematic of the Sallen-Key topology is shown in Figure 4.1. This topology can be used to realize many second-order filters, high-pass or low-pass, as will be discussed later in this chapter. The transfer function of this filter is given by

$$\frac{V_{out}}{V_{in}}(s) = \frac{R_1 R_2}{(C_1 C_2)s^2 + R_1(C_1 + C_2)s + 1}, \tag{4.1}$$

where s is the complex frequency calculated using the Laplace Transform.

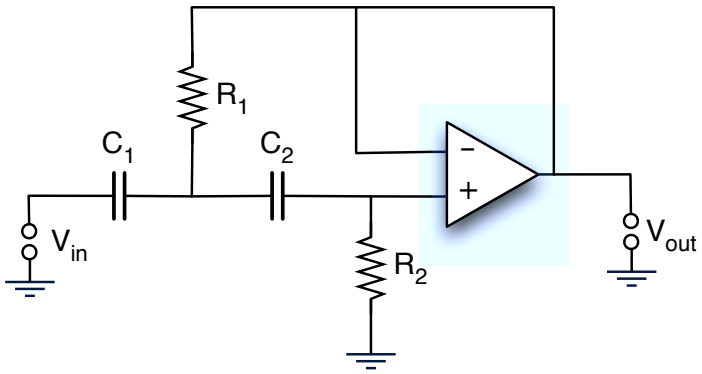

Figure 4.1 Circuit diagram of a second-order low-pass Sallen-Key filter.

4.2.2 Fleischer-Tow Biquad

Fleischer and Tow designed a biquad filter topology that is more complex than the Sallen-Key filter, as shown in Figure 4.2. However, it is quite powerful because it can realize any second order transfer function with the use of only three op-amps [23,24]. This makes it more versatile than the Sallen-Key topology, but requires more elements to realize. The Laplace domain transfer function for this type of filter is given by

$$\frac{V_{out}}{V_{in}}(s) = \frac{\frac{R_8}{R_6}s^2 + \frac{1}{R_1C_1}\left[\frac{R_8}{R_6} - \frac{R_1R_8}{R_4R_7}\right]s + \frac{R_8}{R_3R_5R_7C_1C_2}}{s^2 + \frac{1}{R_1C_1}s + \frac{1}{R_2R_3C_1C_2}\cdot\frac{R_8}{R_7}}. \tag{4.2}$$

The term biquad refers to the fact that the transfer function is a ratio of quadratic functions in s.

Previous research has shown that a Fleischer-Tow biquad topology can be used effectively as a feedback noise controller [25]. For this reason, it was chosen as a possible candidate for the current research.

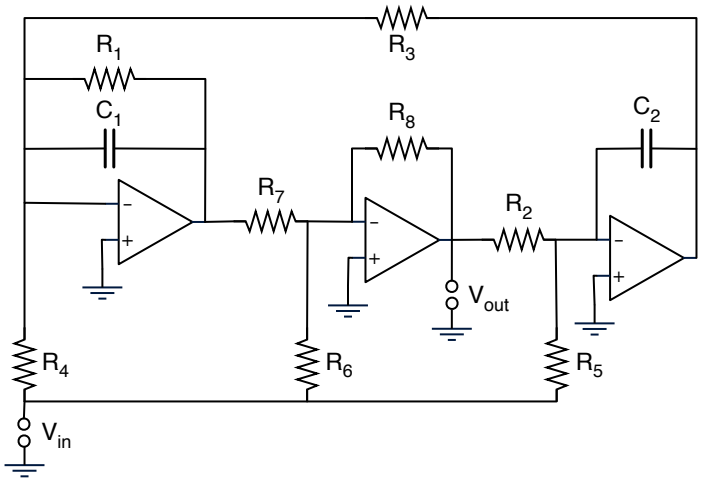

Figure 4.2 Circuit diagram of a Fleischer-Tow biquad filter.

4.2.3 Bach

The second-order low-pass Bach filter topology was chosen for the Chebyshev filters in this research. This topology was chosen over a Sallen-Key topology because it offered more versatility for large ripple width while still allowing reasonable component values. The transfer function of this topology is given by

$$\frac{V_{out}}{V_{in}}(s) = \frac{R_1C_1R_2C_2}{(R_1C_1R_2C_2)s^2 + (R_2C_2)s + 1}. \tag{4.3}$$

Figure 4.3 shows the Bach filter topology.

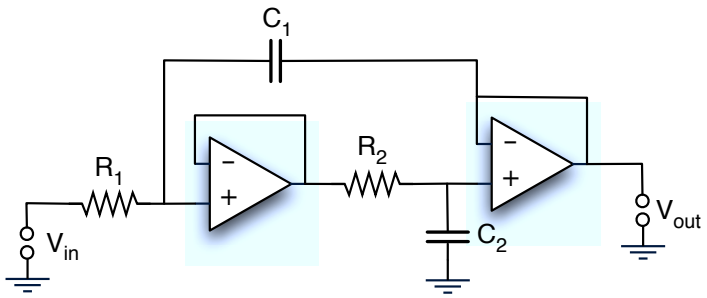

Figure 4.3 Filter topology for a second-order Bach filter.

4.2.4 Differentiator

Differentiator circuits are commonly used in feedback control to control the low-frequency response of the system. Figure 4.4 shows a common implementation of a differentiator circuit. The transfer function of this circuit is given by

$$\frac{V_{out}}{V_{in}}(s) = \frac{s + \frac{1}{R_1 C_1}}{s + \frac{1}{R_2 C_2}}. \tag{4.4}$$

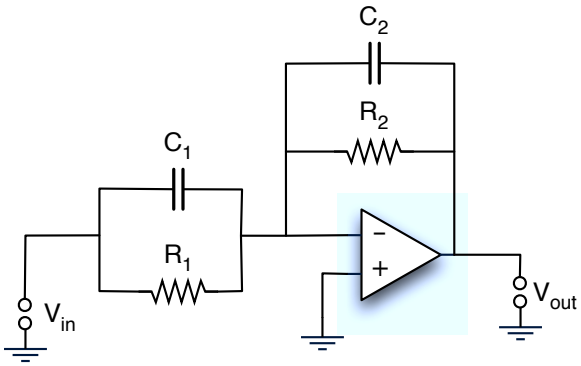

Figure 4.4 Filter topology for a differentiator.

4.2.5 All-Pass

All-pass filters are designed to not affect the magnitude, but simply introduce phase into the system. It may seem counterintuitive that one would intentionally introduce more phase into a system where a flatter phase is desired. However, it can be useful to shift the region of stable phase down in frequency to a region with greater magnitude.

Figure 4.5 shows the topology used for the all-pass filter [26]. The transfer function of this circuit is given by

$$\frac{V_{out}}{V_{in}}(s) = \frac{\frac{s}{R_1C_1} - 1}{\frac{s}{R_1C_1} + 1}. \tag{4.5}$$

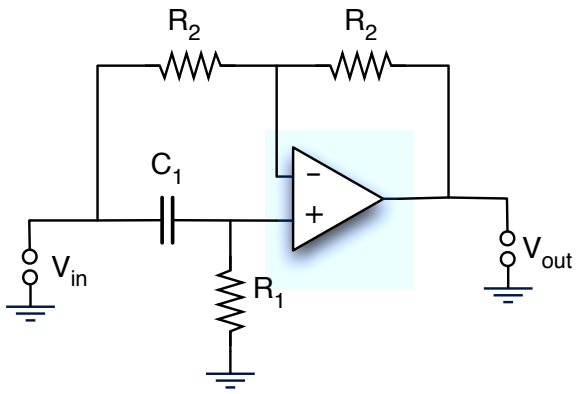

Figure 4.5 Filter topology for an all-pass filter.

4.3 Filter Types

4.3.1 Butterworth

A Butterworth filter is one whose magnitude response is as flat as possible in the pass band. It then decreases monotonically in the stop band. Figure 4.6 shows a second-order Butterworth filter with cutoff frequency at 1000 Hz. The magnitude at the cutoff frequency is 3 dB down from its

maximum gain, and the magnitude decreases at a rate of 12 dB per octave in the stop band. The transfer function of a second-order, low-pass Butterworth filter is given by

$$\frac{V_{out}}{V_{in}}(s) = \frac{G_0}{(\frac{s}{\omega_c})^2 + \sqrt{2}\frac{s}{\omega_c} + 1}. \tag{4.6}$$

G_0 represents the DC gain of the filter, and ω_c represents the cutoff frequency of the filter in radians/second.

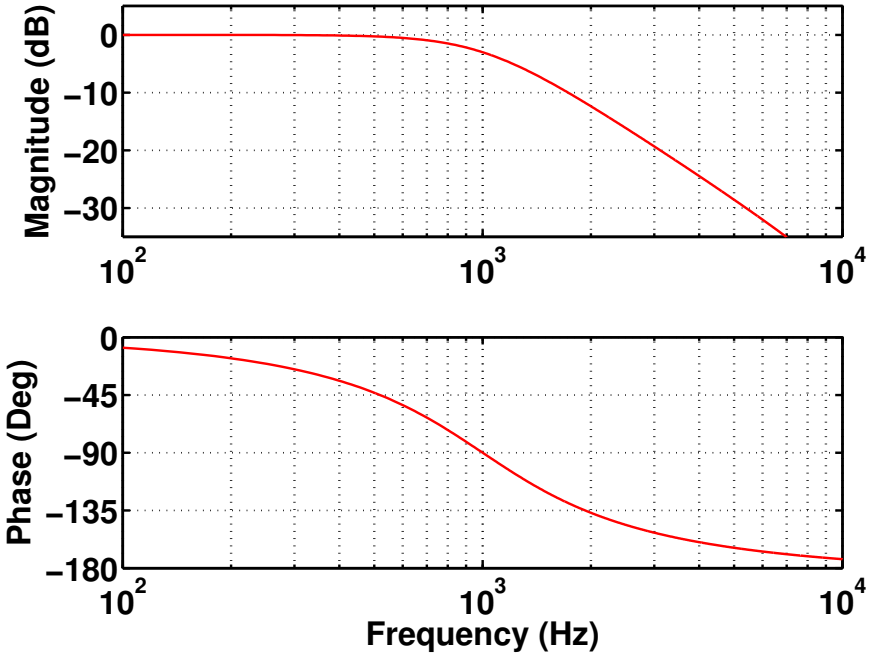

Figure 4.6 Magnitude and phase response of a Butterworth filter.

Butterworth filters have 45 degrees of phase per pole at the cutoff frequency. So, in the case of the 2 pole filter shown, the filter has introduced 90 degrees of phase when the magnitude is only 3 dB below its maximum value. The Butterworth filters used in this research are built using the Sallen-Key topology.

4.3.2 Chebyshev

Chebyshev filters are characterized by a relatively steep rolloff in the stop band, with ripple in the pass band. This ripple is typically an undesired but necessary tradeoff to achieve a steeper rolloff in the stop band. The Chebyshev filters used in this research were two-pole filters, meaning they exhibit only one ripple in the pass band. Chebyshev filters can be defined by their ripple width, or the difference in DC gain and peak gain, and their cutoff frequency, or the frequency at which the magnitude passes through the DC gain level, decreasing into the stop band. The ripple width, in dB, is defined as RW. The variable h is defined as

$$h = tanh\left(\frac{1}{2}sin^{-1}\left(\frac{1}{\sqrt{10^{RW/10}-1}}\right)\right). \tag{4.7}$$

The transfer function of a second-order Chebyshev filter can then be defined in terms of a_i and b_i, where a_i is defined as

$$a_i = \sqrt{\frac{1}{1-h^2} - \frac{1}{2}} \tag{4.8}$$

and b_i is defined as

$$b_i = \frac{1}{2h}\sqrt{h^2+1}. \tag{4.9}$$

The transfer function is then given by

$$\frac{V_{out}}{V_{in}}(s) = \frac{G_0}{\left(\frac{1}{a_i\omega_c}\right)s^2 + \frac{1}{a_i b_i \omega_c}s + 1}. \tag{4.10}$$

G_0 represents the DC gain of the filter, and ω_c represents the cutoff frequency of the filter in radians/second.

Figure 4.7 shows the magnitude and phase response of a two-pole Chebyshev filter. Its cutoff frequency is 1000 Hz and it has 10 dB of ripple in the pass band. It is worth noting that the phase

introduced by a Chebyshev filter is steeper than that of a Butterworth, but a Chebyshev filter can produce a bandpass response in the magnitude of the system.

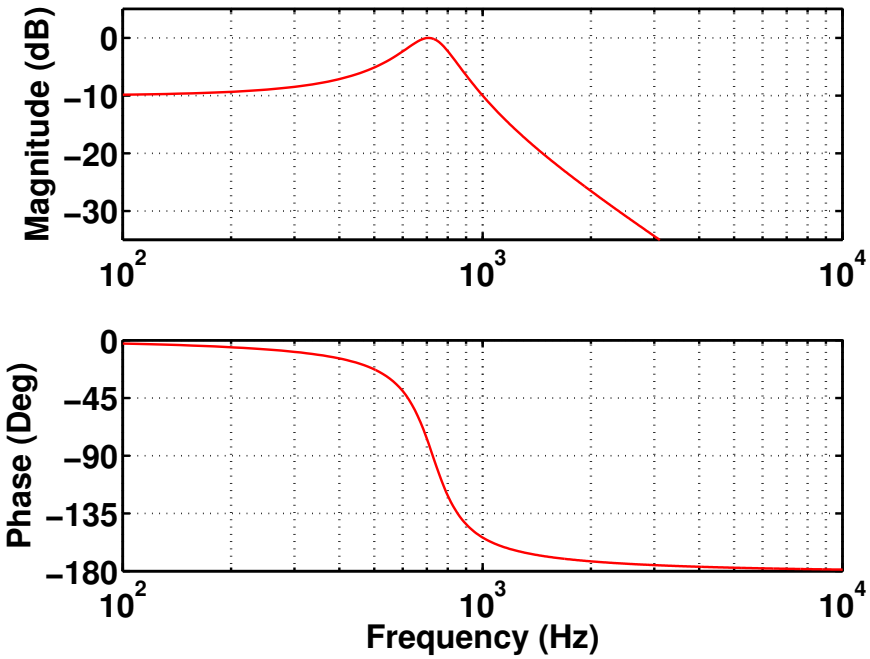

Figure 4.7 Magnitude and phase response of a Chebyshev filter.

4.3.3 Lead compensator

Lead compensators are a popular choice for feedback control design because of their ability to affect a change in phase in some frequency region without affecting the entire frequency range. A lead compensator is designed with two cutoff frequencies, ω_1 and ω_2, which bound the region of increased phase. The transfer function of this filter is given by

$$\frac{V_{out}}{V_{in}}(s) = \frac{s+\omega_1}{s+\omega_2}. \tag{4.11}$$

The region of increased phase also corresponds to a high-pass type response in the magnitude, but outside of this region, the filter has a flat magnitude and phase response, as seen in Figure 4.8. This filter has cutoff frequencies of 100 Hz and 1000 Hz.

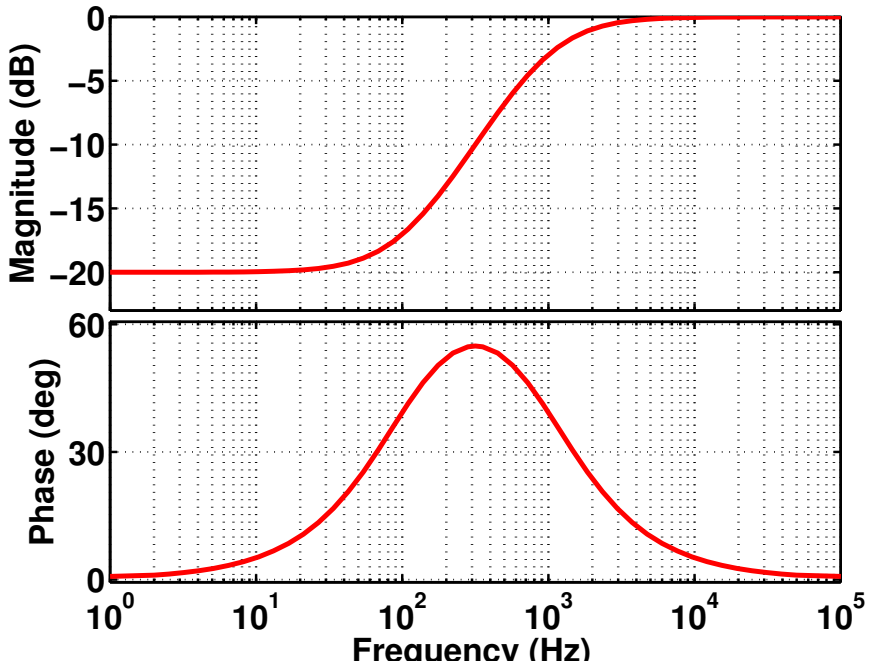

Figure 4.8 Magnitude and phase response of a lead compensator.

4.3.4 All-pass

Figure 4.9 shows that an all-pass filter has a uniform magnitude response. The phase changes similarly to a second-order Butterworth filter, crossing through -90 degrees at the cutoff frequency (1000 Hz). The corresponding transfer function is given by

$$\frac{V_{out}}{V_{in}}(s) = \frac{\frac{s}{\omega_c} - 1}{\frac{s}{\omega_c} + 1}, \tag{4.12}$$

where ω_c represents the cutoff frequency, or the -90 degree phase point of the filter.

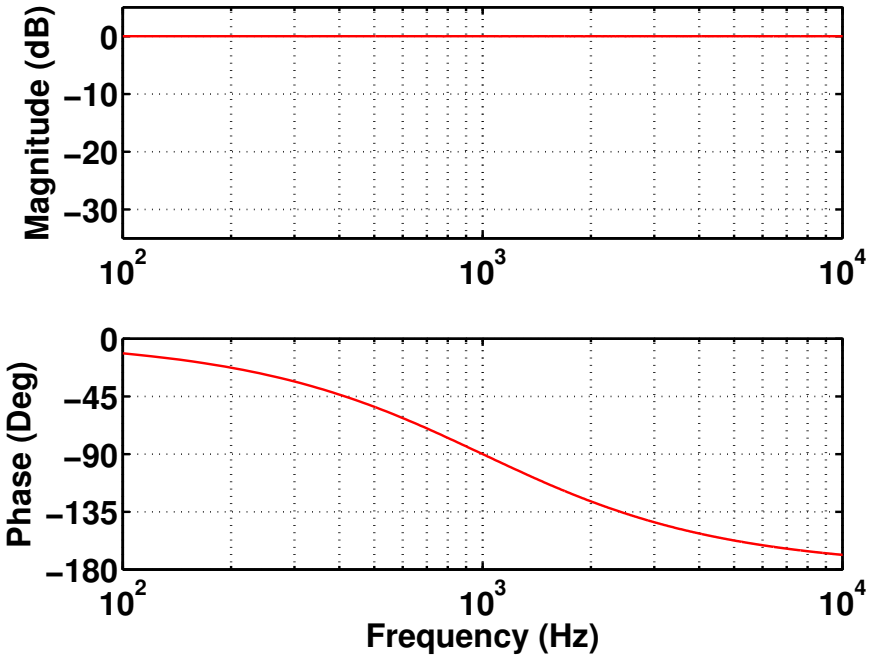

Figure 4.9 Magnitude and phase response of an all-pass filter.

For various aspects of the project, each of these filters was investigated. Ultimately, what led to the best results was a combination of a Chebyshev filter and a lead compensator, as will be outlined in Chapter 5.

Chapter 5

Experimental Setup

5.1 Computer case and fan

The system used in this research consists of a mock computer case with a 60mm axial cooling fan mounted on the top exterior face of the box. The computer case is constructed of aluminum panels, and was constructed to mimic the general size of a typical desktop computer. The case is 16.5 inches tall, 18.5 inches wide, and 8.5 inches deep. Additionally, the inside of the box has been treated with damping material to cut down on resonance effects of the box. There is a hole cut in the side of the box to allow for air flow as well as cable throughput. A photo of the mock computer case can be seen in Figure 5.1.

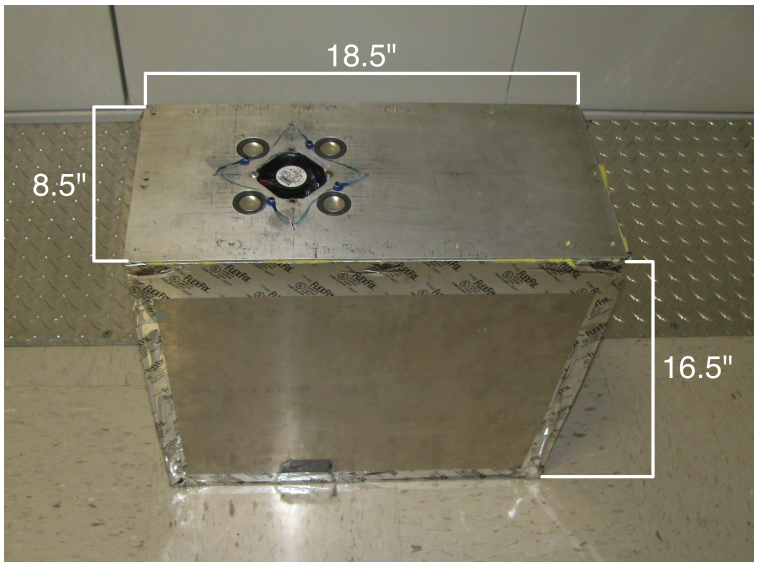

Figure 5.1 A photo of the mock computer case.

5.2 Control sources and error sensors

The fan is surrounded by four loudspeakers which act as secondary sources for the controller. These loudspeakers are one-inch high-excursion drivers. PVC caps have been applied to the back side of the loudspeakers to act as enclosures to maximize output, as seen in Figure 5.2. The amplitude response of the loudspeakers has a peak at approximately 300 Hz, and a relatively flat response ($\pm$ 2.5 dB) between 500 Hz and 6000 Hz, as previously shown in Figure 3.5. The loudspeakers are placed symmetrically around the fan, and as close to the fan as the geometry allows. Four small electret microphones also surround the fan. They are placed in specific locations to maximize global noise control, as discussed in Section 2.2.

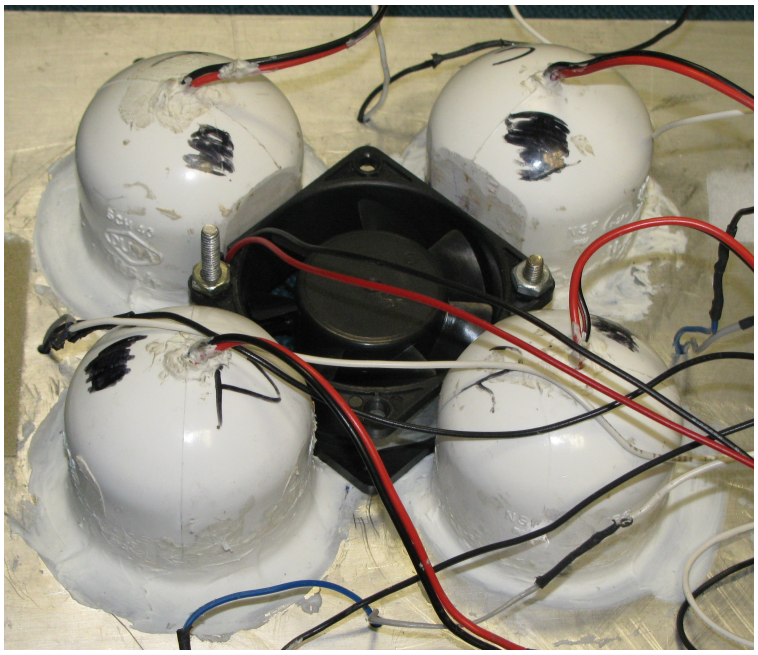

Figure 5.2 A photo of the rear of the fan showing the PVC loudspeaker enclosures.

5.3 Measurements

Far-field measurements for this research were performed in an anechoic chamber using a semi-circular microphone array, as seen in Figure 5.3. Thirteen 1/2" microphones are placed at 15 degree increments, and the boom is rotated about the vertical axis at 15 degree increments. This provided sound pressure measurements covering an entire hemisphere surrounding the fan. Sound power radiation from the fan was then calculated from these measurements. Sound power is a measure of acoustic intensity over area. However, since the microphones are spaced at equal angles around the boom, the microphones toward the bottom of the boom essentially cover a larger area. Therefore, the pressure was measured at each microphone, and a weighted sum was used to calculate the sound power over the hemisphere [5].

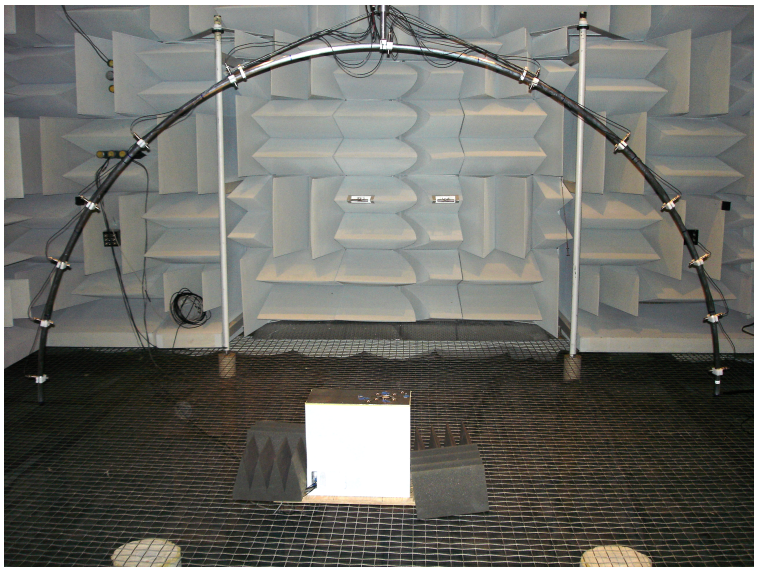

Figure 5.3 A boom microphone array used for far-field measurements.

5.4 Control filters

Multiple types of control filters were used throughout the research. Five filters were selected to appear in this thesis. They will be referred to as Filters #1 - #5. Their physical construction will be outlined in this section, and the magnitude and phase response of each filter will also be shown. The corresponding open-loop response, as well as experimental results are shown in Chapter 6.

5.4.1 Filter #1

The first filter is designed using the Fleischer-Tow biquad topology. This type of filter was chosen as a good candidate initially because of its versatility. Being a two-pole filter, it introduces less phase than a higher order filter would. However, it is also not able to cause as steep of a rolloff in the stop band of the filter. Filter #1 was designed to have a bandpass magnitude response centered around 900 Hz. This frequency was chosen so the control region would lie between the blade passage frequency (BPF) of the fan (650 Hz) and its second harmonic (1300 Hz). A circuit diagram

for this filter can be seen in Figure 5.4, and a corresponding Bode plot is found in Figure 5.5.

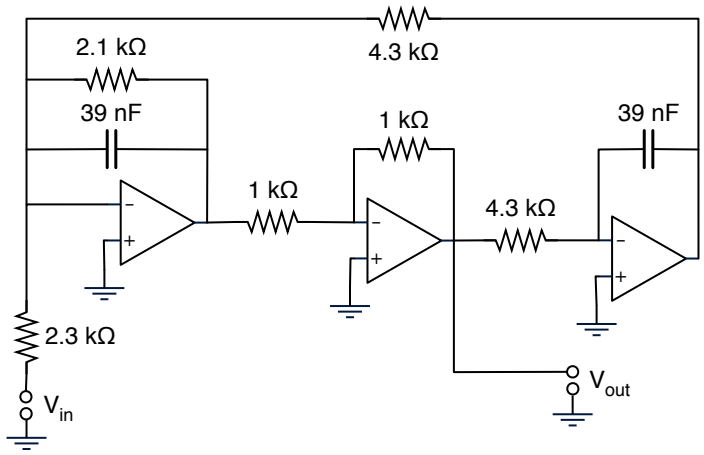

Figure 5.4 A circuit diagram for Filter #1.

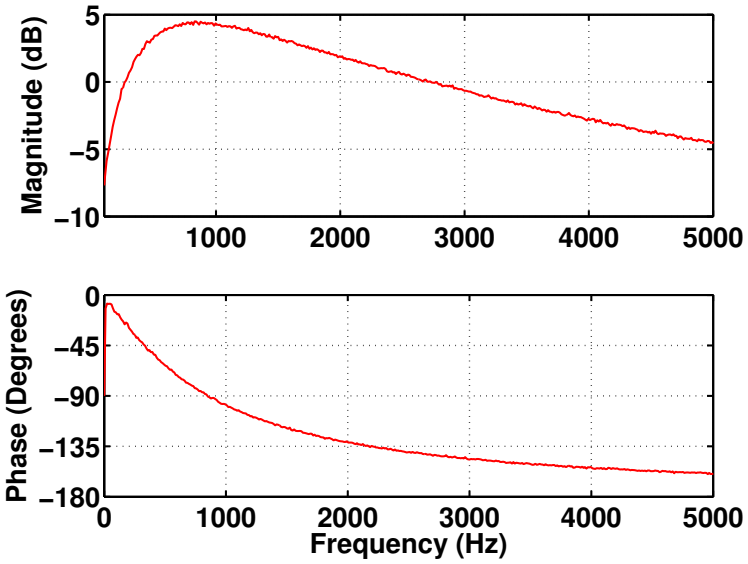

Figure 5.5 Magnitude and phase response of Filter #1.

Preliminary results are shown for the Fleischer-Tow biquad in Chaper 6. However, due to delay in the system, it was determined early on that a higher order filter would be necessary for the purposes of this research. However, using a higher-order filter imposes two restrictions on the

control system. First, the higher order of the control filter will cause a corresponding steepness in the open-loop phase. Therefore, a higher-order control filter effectively shrinks the frequency range of control. Second, there is not a simple filter topology which can be applied to reliably achieve any specific higher-order transfer function, such as the Fleischer-Tow biquad. Therefore, the filters used later in this research consist of combinations of well-known filter types for ease of design and implementation.

5.4.2 Filter #2

The second filter to be used is a combination of a one-pole high-pass filter and a four-pole low-pass Sallen-Key Butterworth filter. The cutoff frequencies are 500 Hz and 1700 Hz, respectively. This combination was chosen because the previous filter demonstrated greater instability at higher frequencies. Therefore, a steeper rolloff was chosen for the upper end of the control region rather than for the lower end. A circuit diagram of the filter is shown in Figure 5.6 and the corresponding Bode plot is shown in Figure 5.7.

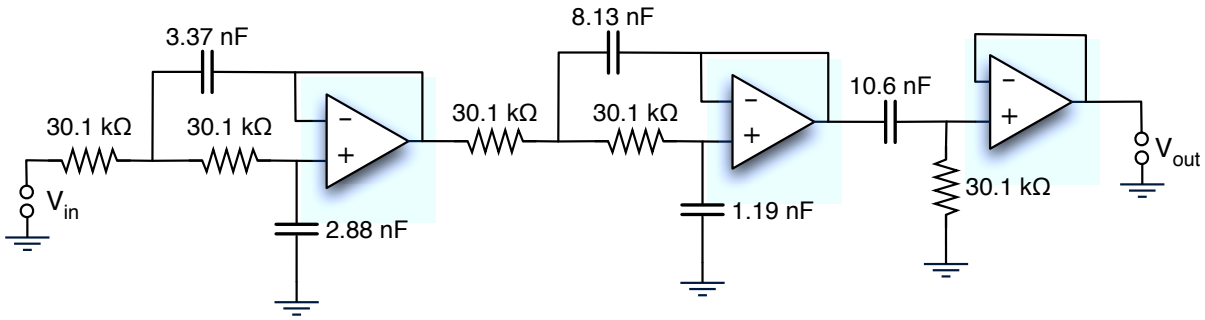

Figure 5.6 Circuit diagram for Filter #2.

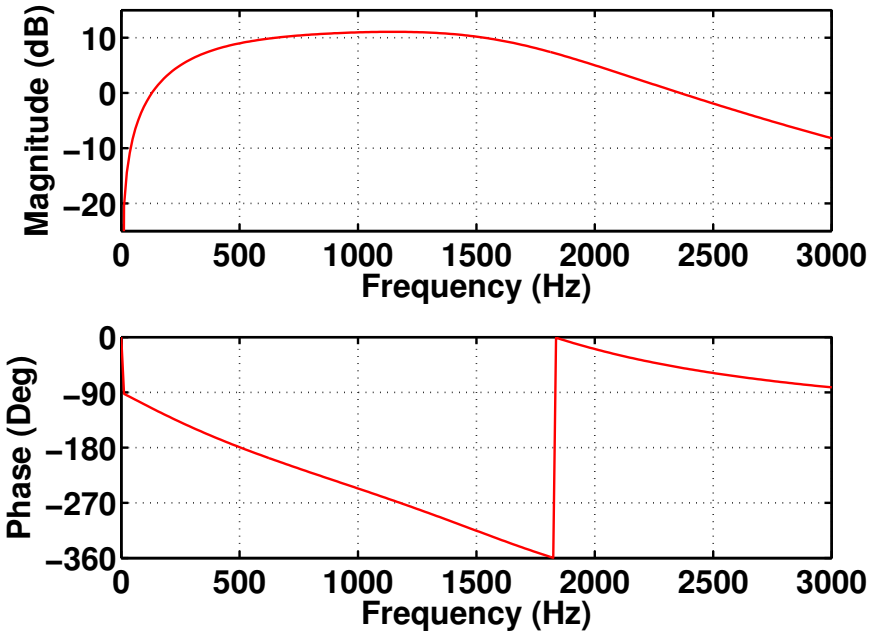

Figure 5.7 Magnitude and phase response of Filter #2.

5.4.3 Filter #3

As discussed in Section 4.1, it is not possible to affect the magnitude of an analog filter without also affecting the phase. In the case of a Butterworth filter, one half of the phase change introduced by the filter occurs in the pass band, as can be seen in Figure 4.6 . Because this type of filter introduces so much phase before any significant reduction in magnitude, it was decided that a combination of Butterworth filters would not be practical for this project. However, it is possible to achieve a bandpass response using the pass-band ripple of a Chebyshev filter without introducing as much phase as with a combination of low-pass and high-pass filters.

The next configuration was therefore one which incorporated a Chebyshev filter with a relatively large amount of ripple in the passband. The ripple in the passband would be used to affect a bandpass response in the control region. A Chebyshev filter also offers steeper rolloff in the stop band than would exist with a comparable Butterworth filter. In the case of a typical two-pole

low-pass filter, the 90 degree phase point happens around the cutoff frequency. In the case of a Chebyshev filter, since the bandpass response of the ripple happens below the cutoff frequency, as can be seen in Figure 4.7, it allows for a desirable trade off of magnitude shaping without introducing excessive phase.

The high-frequency rolloff of a Chebyshev filter is significant. However, there is not enough rolloff at low frequencies to avoid amplification below the control band. For this reason, the Chebyshev filter was combined with a two-pole high-pass Butterworth filter. This was designed to minimize amplification below the control band. The Chebyshev filter has a cutoff frequency of 2100 Hz with 12 dB of ripple in the passband. The Butterworth filter has a cutoff frequency of 3500 Hz. The circuit diagram of this filter can be seen in Figure 5.8 and the corresponding frequency response is shown in Figure 5.9

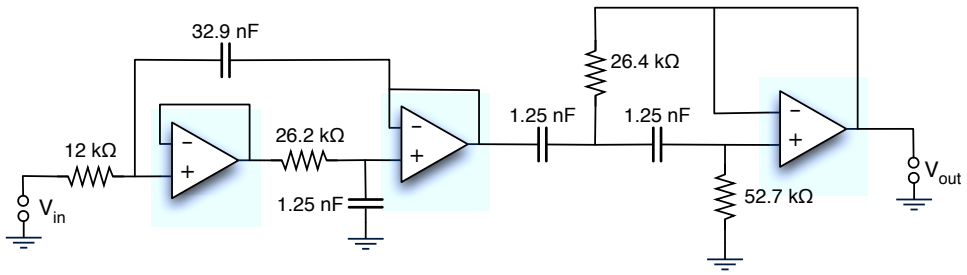

Figure 5.8 Circuit diagram for Filter #3.

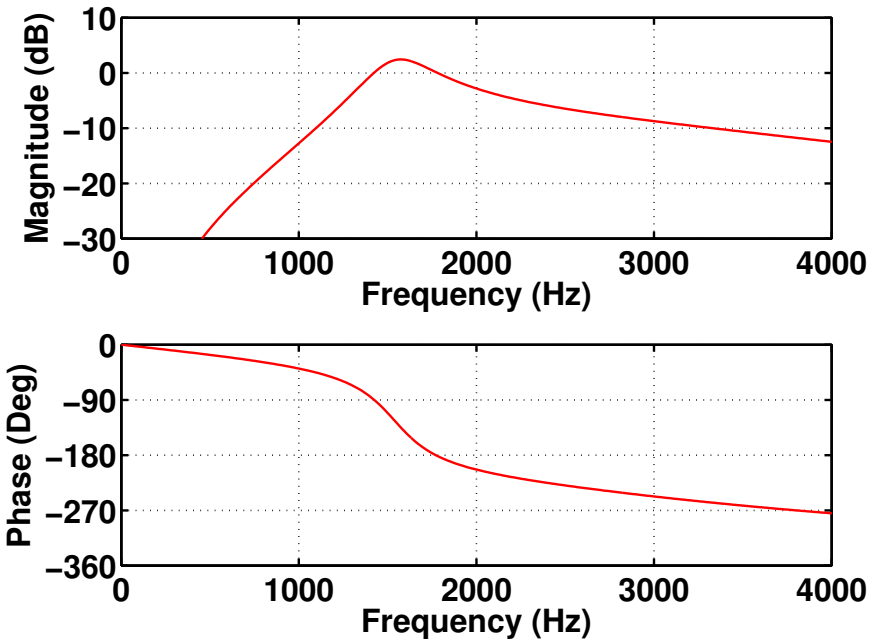

Figure 5.9 Magnitude and phase response of Filter #3.

5.4.4 Filter #4

The relatively high cutoff frequency of the Butterworth filter in the previous example caused undue amplification above the frequency range of control. To alleviate this, a one-pole high-pass filter was combined with a Chebyshev filter. This allowed for a flatter phase response throughout the frequency range of control. However, this resulted in a filter whose region of maximum magnitude did not correspond to the region of phase which would cause attenuation. For this reason, an all-pass filter was also introduced to simply shift the region of desirable phase to the frequency range of maximum amplitude. The Chebyshev filter has a cutoff frequency of 1500 Hz with 12 dB of ripple in the passband. The high pass filter has a cutoff frequency of 1650 Hz, and the all-pass filter has a cutoff frequency of 600 Hz. Figure 5.10 shows the block diagram for the entire filter, and the corresponding frequency response can be seen in Figure 5.11.

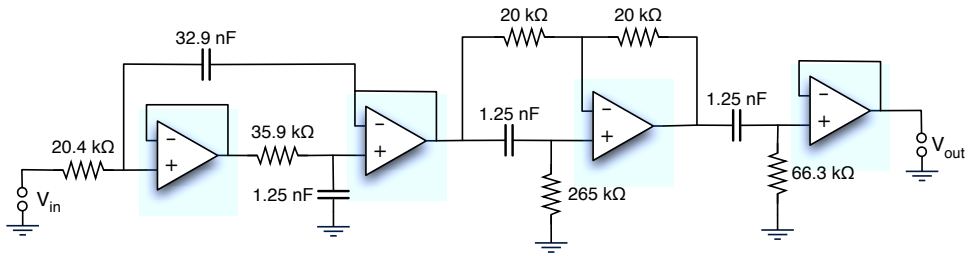

Figure 5.10 Circuit diagram for Filter #4.

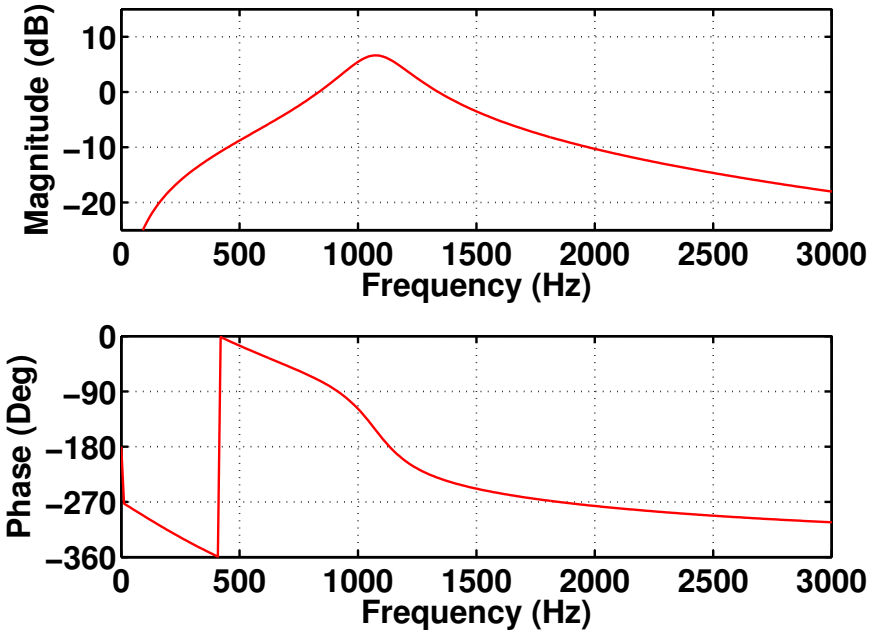

Figure 5.11 Magnitude and phase response of Filter #4.

5.4.5 Filter #5

Filter #5 consists of a Chebyshev filter combined with a lead compensator. This filter was chosen to demonstrate the ability to design similar filters in different frequency regions. The fan noise in this research has significant energy at low frequencies, so this filter was designed at a frequency region below the BPF to attenuate the loudest frequency region. The Chebyshev filter has a cutoff frequency of 700 Hz, and the lead compensator has cutoff frequencies of 100 Hz and 2000 Hz.

Figure 5.12 shows the block diagram for the combined filter, and the corresponding frequency response can be seen in Figure 5.13.

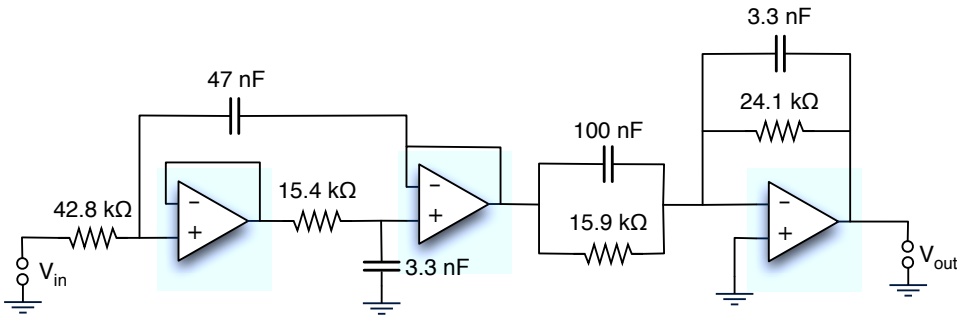

Figure 5.12 Circuit diagram for Filter #5.

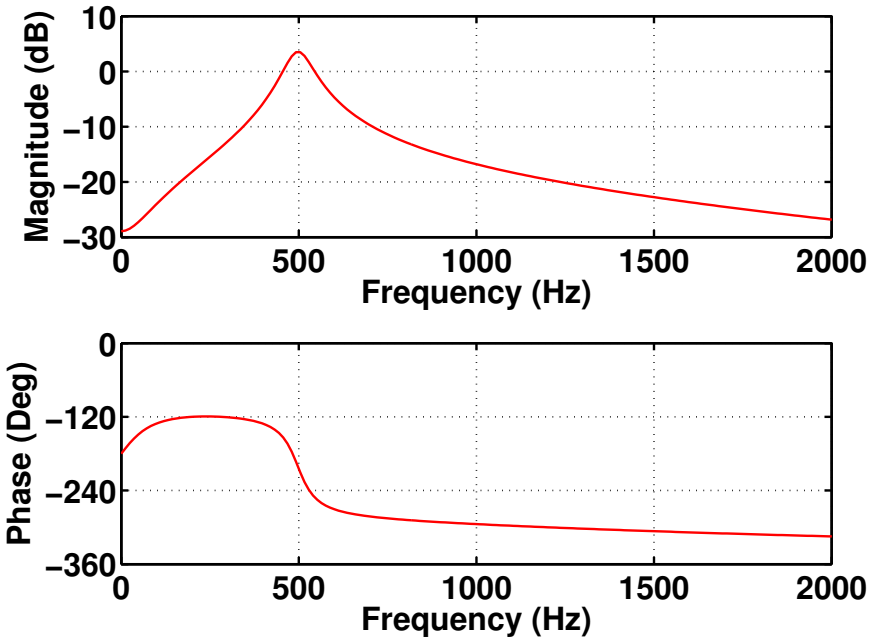

Figure 5.13 Magnitude and phase response of Filter #5.

5.4.6 Summary

The filters chosen in the early part of this research all created too much noise amplification outside the region of control to make them feasible options for broadband noise control. Many attempts were made to alleviate this, and the filters which yielded the greatest overall attenuation without excessive amplification were Filter #4 and Filter #5. Because of this, Chapter 6 will show near-field analog control results for each filter detailed in Chapter 5, but far-field and digital hybrid results will only be shown for Filters #4 and #5.

Chapter 6

Results and Analysis

6.1 Results overview

Results for the analog controller are shown for multiple configurations. Multiple types of filters were tested, and their benefits and drawbacks were investigated. Initial tests were performed in a SISO configuration, and attenuation performance was evaluated near the fan at the error sensor. Additional testing was then performed to assess far-field performance of the controller. Far-field results will be shown for Filter #4 and Filter #5. In this case, attenuation results will be shown at the error sensor, as well as in the far field of the fan assembly.

A numerical model has been developed for the purpose of designing a feedback controller, as well as determining the benefit of a MIMO controller. Theoretical attenuation was modeled numerically based on the filter response as well as the response of the plant. These results will be presented along with those measured to demonstrate the accuracy of the model. Discrepancies between measured attenuation and predicted attenuation will also be investigated.

The analog broadband controller will then be combined with the existing digital tonal controller. This will show viability of using both controllers simultaneously, as well as demonstrate

any improvement in performance over the tonal controller alone. The configuration where both controllers are incorporated simultaneously will be referred to as hybrid control. Hybrid results will be shown for Filter #4 and Filter #5.

6.2 MIMO Control

A numerical model was developed to determine the viability of a MIMO controller. In Section 3.5 the principle of a relative gain matrix was explained. This can be used to assess the level of interaction between each input and output in a multi-channel system. The relative gain matrix for the current system is given by

$$\begin{bmatrix} y_1 \\ y_2 \\ y_3 \\ y_4 \end{bmatrix} = \begin{bmatrix} 0.0 & -7.3 & -11.9 & -10.5 \\ -19.6 & 0.0 & -13.0 & -20.4 \\ -21.8 & -13.5 & 0.0 & -11.8 \\ -13.8 & -15.8 & -16.0 & 0.0 \end{bmatrix} \otimes \begin{bmatrix} u_1 \\ u_2 \\ u_3 \\ u_4 \end{bmatrix}. \tag{6.1}$$

The matrix is presented in decibels, and the values shown represent the maximum values of the respective impulse responses. This is done because the shape of the impulse responses is not significantly different between the elements, therefore the magnitude difference is the key trait to be investigated. Each row has been normalized to the diagonal element in that row to show the amount of interaction between a given loudspeaker and every microphone, relative to the one closest to it. This equation demonstrates that the level of interaction of these off-diagonal channels is significantly lower than the diagonal elements, typically in excess of 10 dB below the level of interaction with the closest microphone. This suggests that a MIMO type controller is not necessary to ensure stable control.

The frequency response of the these off-diagonal elements also gives some insight into the possible need for a MIMO controller. As demonstrated above, the magnitude response of the off-diagonal elements is significantly lower than the diagonal element. The phase response shows

that the phase is also significantly different between the four responses. The increased acoustic delay between the loudspeaker and microphone manifests as a steeper phase. This means that any controller designed to account for the off-diagonal elements would need to be at very low frequencies because of these differences in phase.

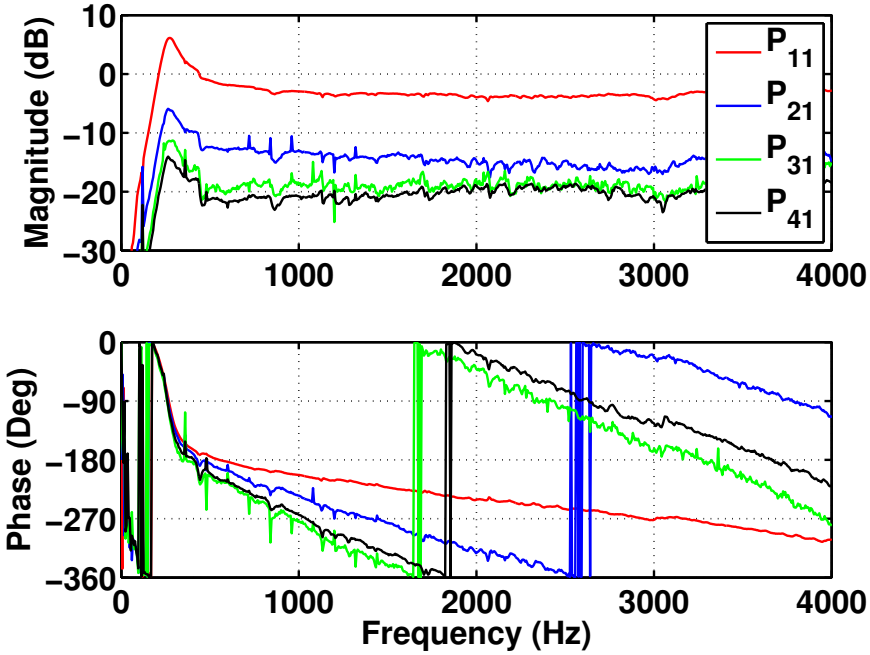

Figure 6.1 Magnitude and phase response of the MIMO system.

Results from the numerical model confirm that the use of a MIMO controller does not enhance the performance of the system. The noise introduced into the system by incorporating the off-diagonal channels far outweighed any possible performance improvement.

6.3 Near-field broadband control

6.3.1 Filter #1

Figure 6.2 shows the fan noise spectrum with and without control using Filter #1. The controller attenuates the noise between about 500 Hz and 2000 Hz. However, there is excessive amplification out of band. This is due to the acoustic delay in the system which introduces increasing phase at higher frequencies, and the rolloff of this two-pole filter is not sufficient to avoid amplification out of band. The controller also introduces a peak around 300 Hz that is not present without the controller. This corresponds to a resonance of the loudspeaker.

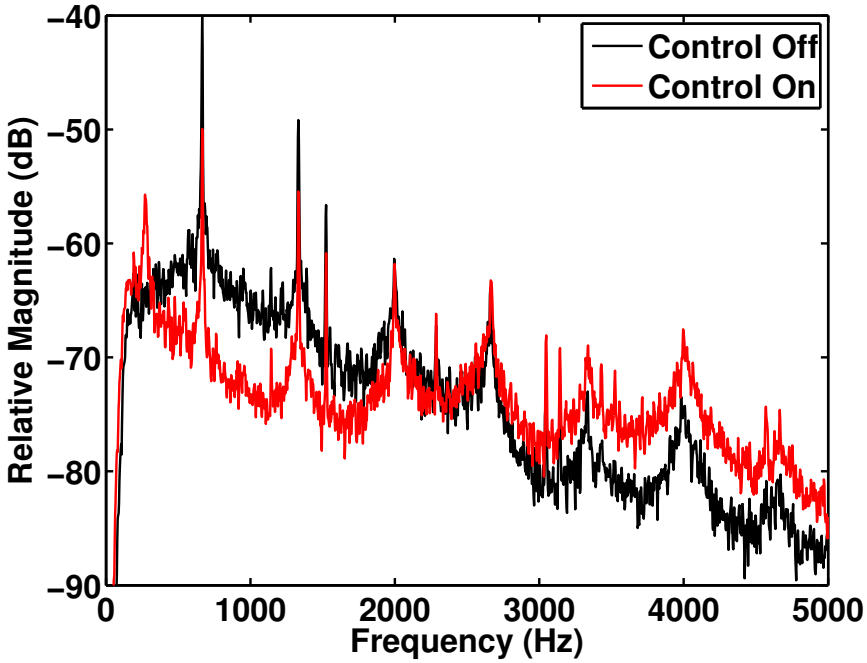

Figure 6.2 Control performance of Filter #1.

6.3.2 Filter #2

Filter #2 consists of a combination of high-pass and low-pass filters constructed using the Sallen-Key topology. This was chosen to achieve independent control over cutoff frequency and rolloff

steepness for the lower end and the upper end of the control region. Figure 6.3 shows the sound pressure level with and without control using Filter #2. Figure 6.3 illustrates that this filter offered as much as 6 dB of noise reduction in the band of control, but at the expense of amplifying the noise out of band. Listening experiments confirmed that the noise amplification out of band made any attenuation unnoticeable.

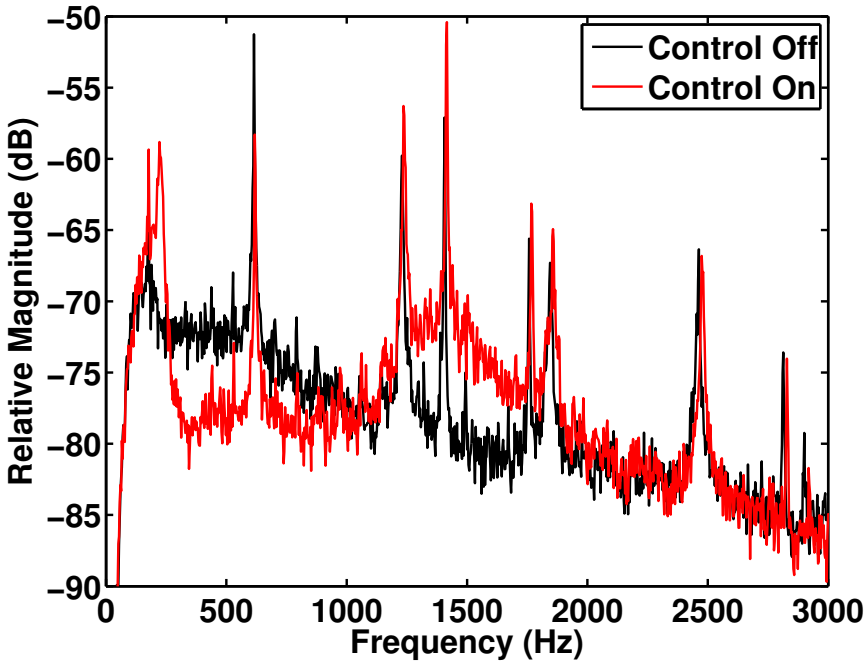

Figure 6.3 Control performance of Filter #2.

Figure 6.4 shows the magnitude and phase of the entire open-loop system when combined with the plant. This illustrates that the region of desirable phase lies between about 350 Hz and 800 Hz. However, the region where the loop gain magnitude is greater than unity spans to much higher frequencies. This explains why this controller augmented the noise above the control band and why it is not an acceptable controller. It is also worth noting that the frequency range of control is smaller than with Filter #1. This is due to the increased order of the control filter. The steeper phase introduced by a higher-order filter effectively shrinks the region of desirable phase.

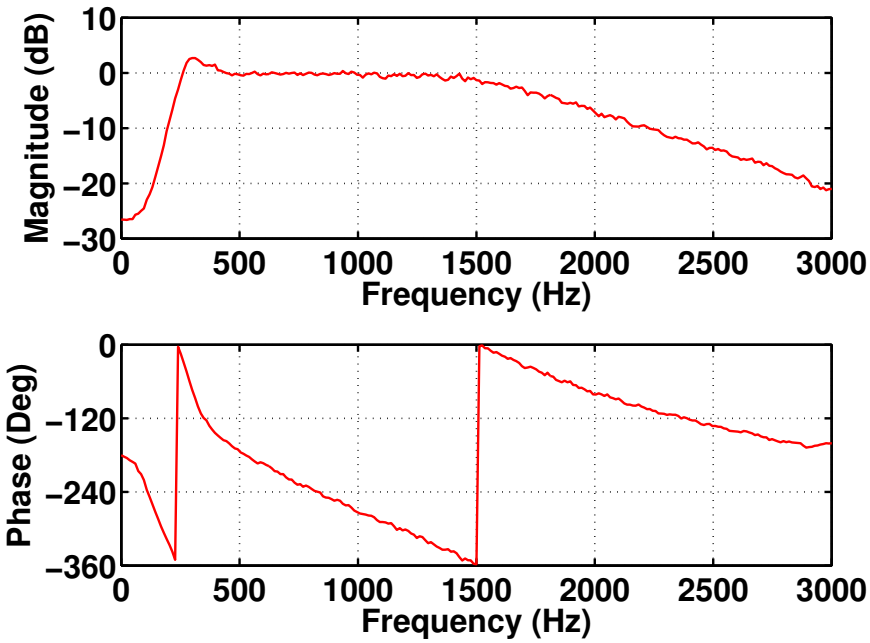

Figure 6.4 Open-loop frequency response including Filter #2.

Figure 6.5 shows a comparison of predicted control performance to measured control performance. This illustrates that the numerical model accurately predicts the performance of the controller. It also shows that this filter does not offer a steep enough rolloff at high frequencies for the amount of phase it is introducing. It is worth noting that the large spikes in the measured attenuation are due to slight shifting of the BPF between measurements, which is sometimes unavoidable.

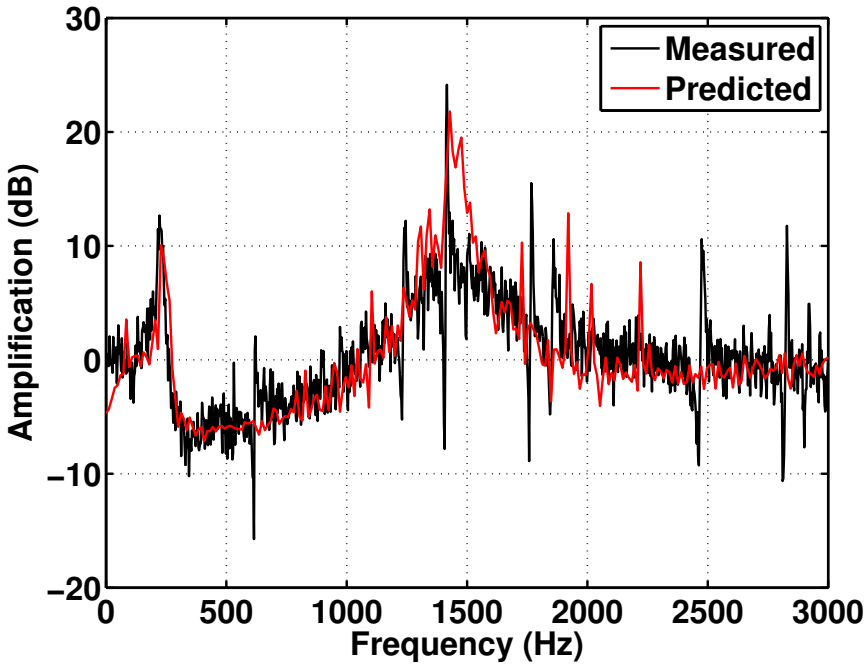

Figure 6.5 Prediction of control performance of Filter #2.

6.3.3 Filter #3

Filter #3 combines a low-pass Chebyshev filter with a high-pass Butterworth filter. This was done to achieve a bandpass response in a smaller frequency range while introducing less phase change than the previous filters. Figure 6.6 shows a comparison of the spectrum with and without noise control. The control band was designed at higher frequencies than the previous two configurations. This was to verify that this type of controller could be designed at different frequency ranges. It was designed to lie between the second harmonic and third harmonic of the BPF, between 1400 Hz and 1850 Hz. This filter offered as much as 5 dB of control in the control band. However, once again, the amplification at frequencies above the control band caused any attenuation to be unnoticeable. Inspection of the open-loop frequency response in Figure 6.7 reveals that the region of greater than unity gain corresponds well to the region of desirable phase. However, the high cutoff frequency of the high-pass filter, 3500 Hz, caused the rolloff above the control band, 1400

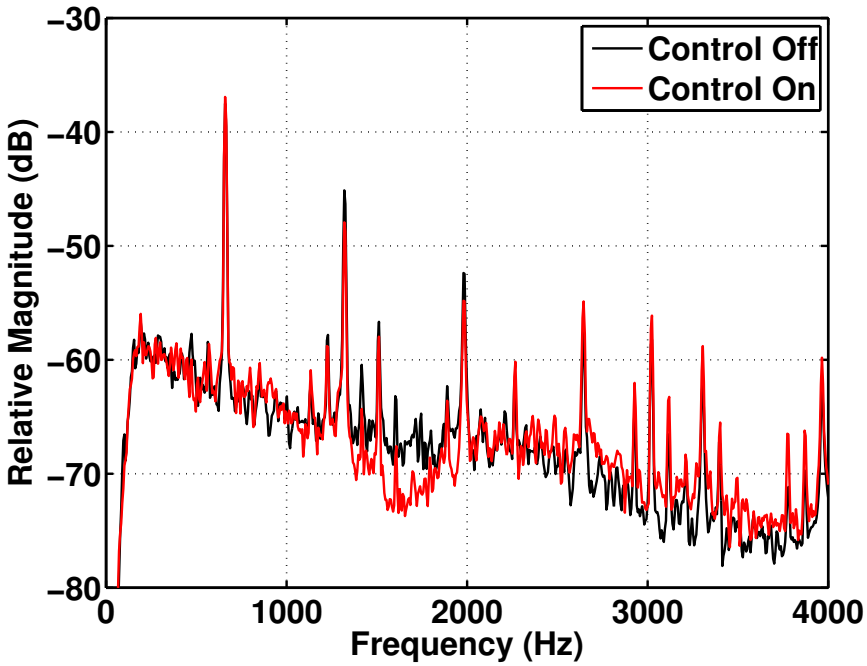

Figure 6.6 Control performance of Filter #3.

Hz to 1850 Hz, to be more gradual.

Figure 6.8 shows, once again, that the model accurately predicts performance of this filter. This controller offers 5 dB of reduction at most in the control band, but it amplifies the noise level by as much as 3 dB out of band.

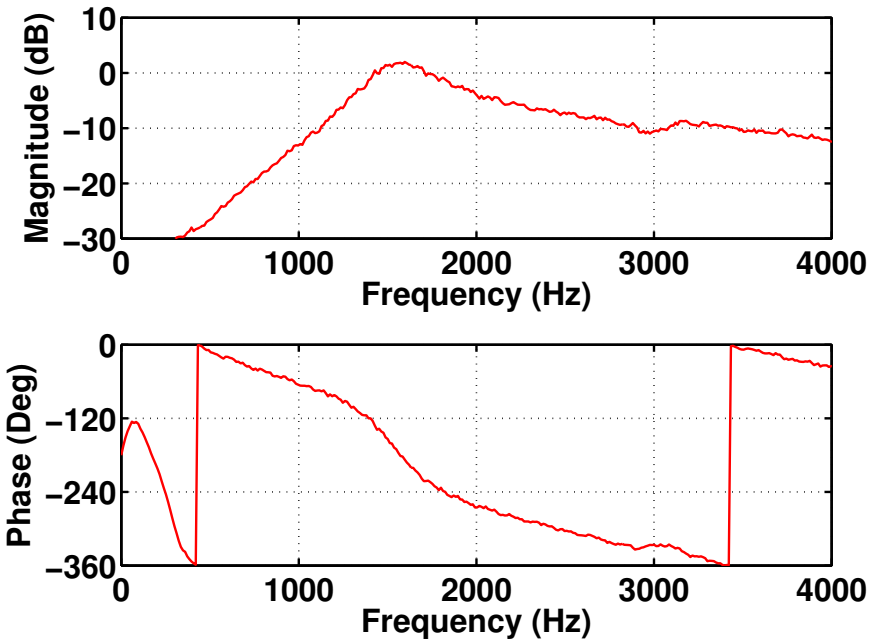

Figure 6.7 Open-loop frequency response including Filter #3.

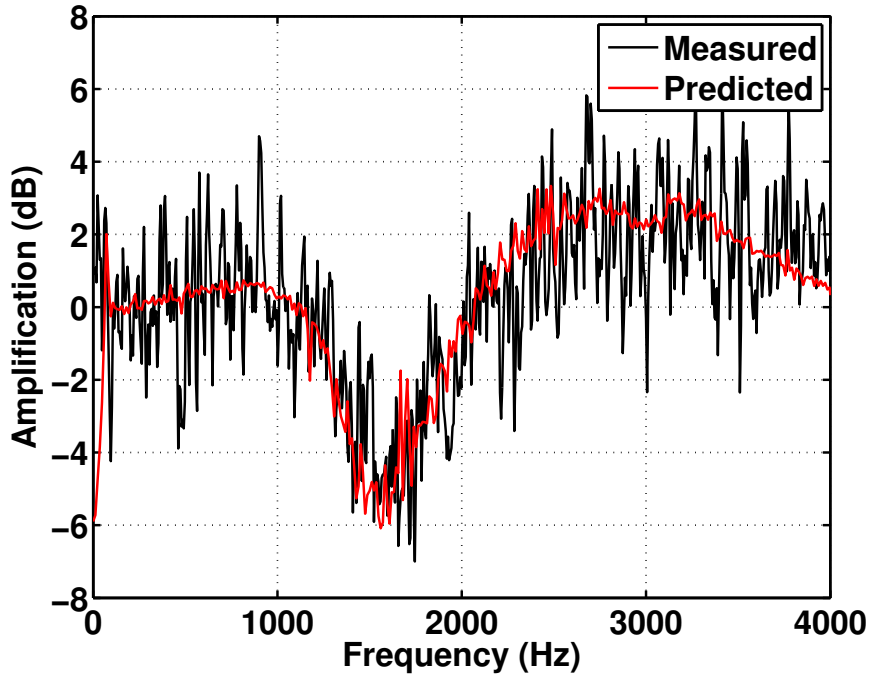

Figure 6.8 Prediction of control performance of Filter #3.

6.3.4 Filter #4

Filter #4 combined a low-pass Chebyshev filter with a high-pass filter and an all-pass filter. This filter was designed with steep rolloffs outside of the control band to combat amplification of the noise in this region. The control region for this filter was designed to be between the BPF of the fan and the second harmonic of the BPF, or between 650 Hz and 1300 Hz. Figure 6.9 illustrates that, at the error sensor, this filter is able to attenuate the noise by as much as 5 dB in the control band without amplifying the out of band noise significantly. Figure 6.10 illustrates why this is possible. The combination of filters offers a relatively steep rolloff both above and below the frequency range of control, and this range is centered around the region of desirable phase.

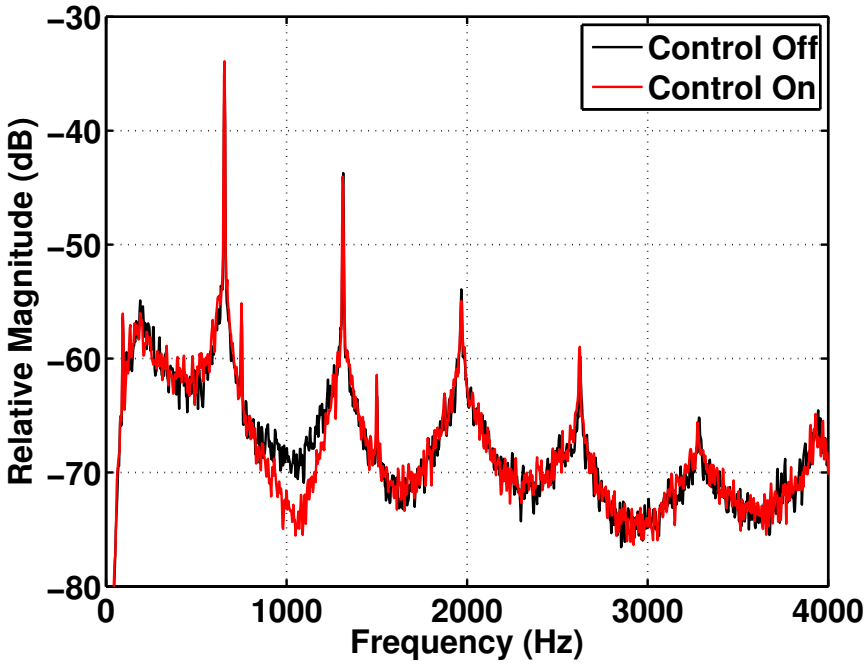

Figure 6.9 Control performance of Filter #4.

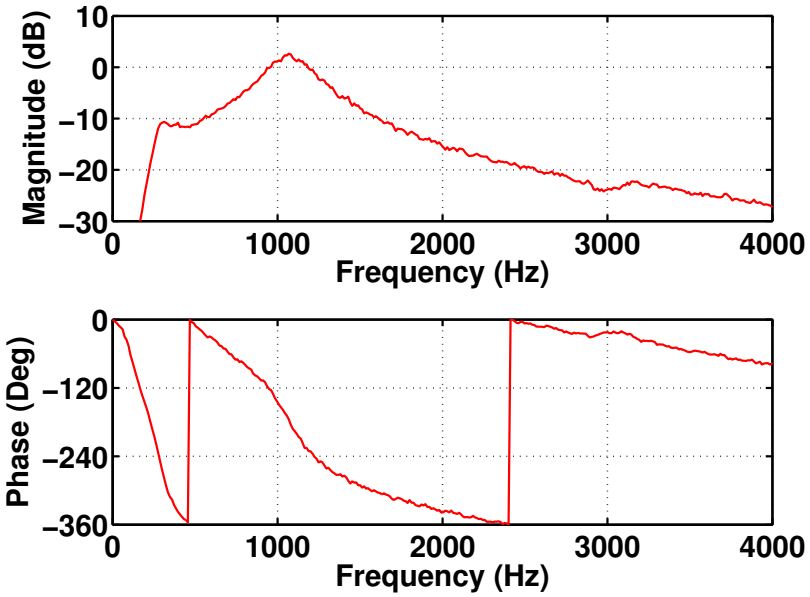

Figure 6.10 Open-loop frequency response including Filter #4.

Figure 6.11 illustrates that this filter offers nearly as much attenuation as the previous filter while causing less amplification out of band.

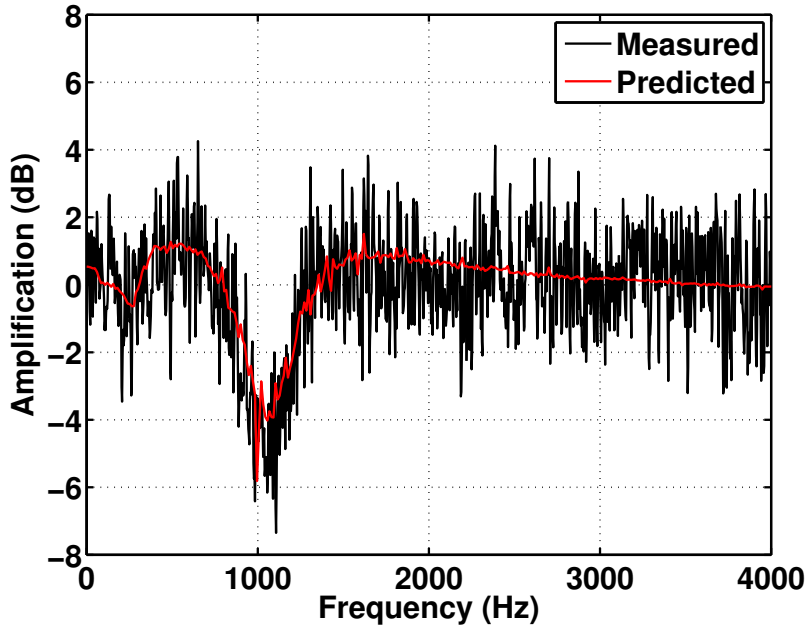

Figure 6.11 Prediction of control performance of Filter #4.

6.3.5 Filter #5

Filter #5 was designed to attenuate noise below the BPF of the fan. Figure 6.12 shows that this controller was able to attenuate noise between 400 and 650 Hz, while boosting between the BPF and the second harmonic of the BPF, as well as a small region below the control region. This region of control was chosen because the sound level was higher at low frequencies. The open-loop response in Figure 6.13 demonstrates that the region of desirable phase corresponds well to the region of highest magnitude. It is also apparent that this lower frequency range is closer to the resonance of the loudspeaker, which accounts for an increased amount of amplification below the control region, as compared to Filter #4.

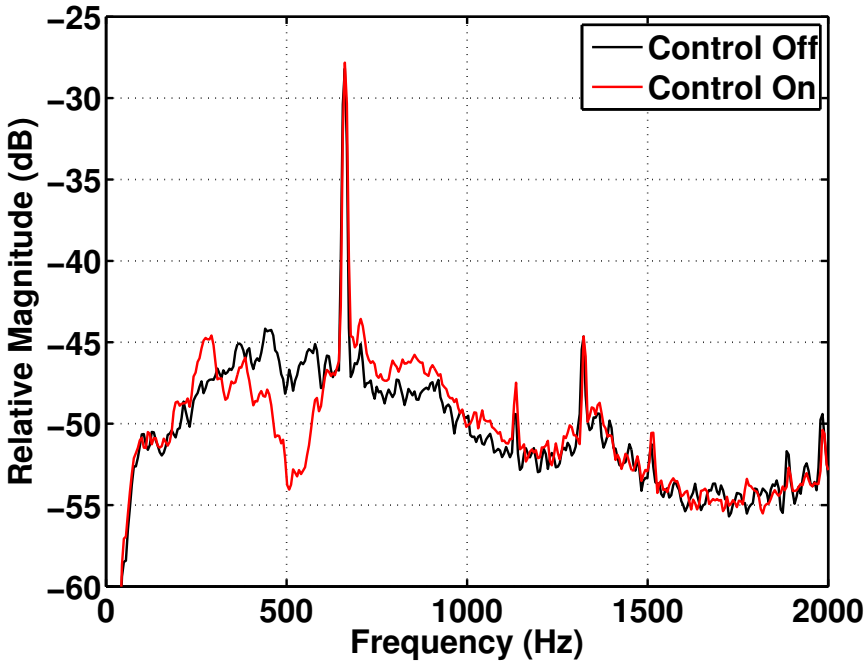

Figure 6.12 Control performance of Filter #5.

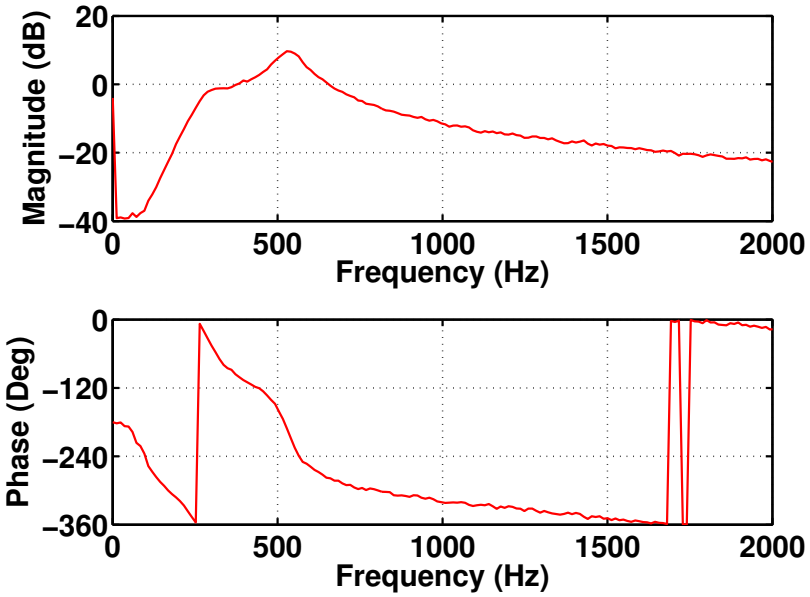

Figure 6.13 Open-loop frequency response including Filter #5.

Figure 6.14 illustrates that this filter is able to attenuate the noise by as much as 7 dB in the control band. However, it amplifies the noise by as much as 3 dB below the control band, due to the resonance of the loudspeaker.

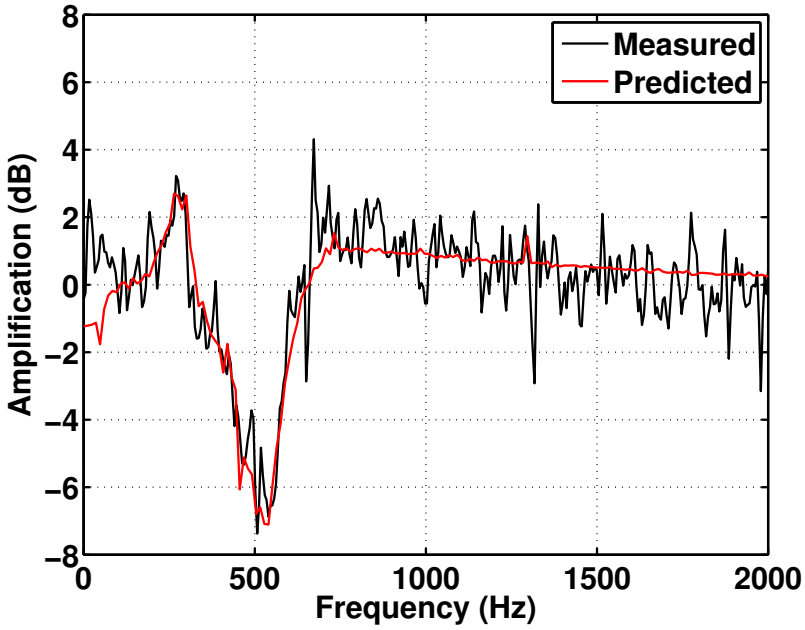

Figure 6.14 Prediction of control performance of Filter #5.

6.4 Far-field broadband control

Previous research has shown that tonal noise control using only properly placed near-field sensors and actuators can translate well to the far field [4, 7]. This is important because it is assumed that the user position of a system such as this will be far from the fan. However, a system requiring any type of sensor in the far-field would not be viable. Therefore, it was necessary to study whether or not broadband attenuation would translate to the far field of the fan as well. Filter #4 was determined to be the best candidate for far-field testing. Therefore, all results presented in this section will be for Filter #4.

Figure 6.15 is a plot of the global sound power radiated from the fan measured on a hemisphere above the fan. This figure illustrates that the attenuation observed near the fan at the error sensor has translated well to the far field of the fan. However, the far-field sound power has been amplified more than predicted outside of the control band. Figure 6.16 shows that, while the model predicts

no more than 1 dB of amplification outside the control band, the measurement indicates that it was actually amplified as much as 4 dB at frequencies below the control band.

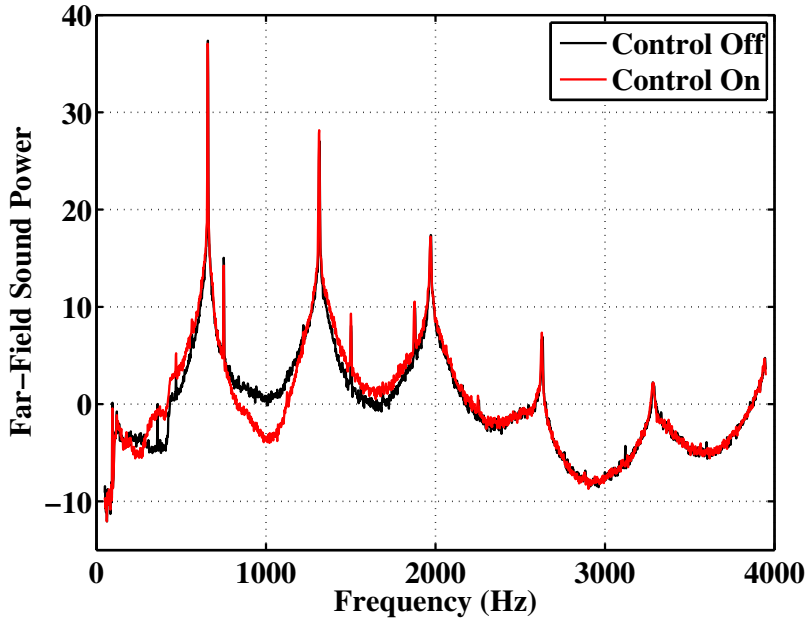

Figure 6.15 Far-field control performance using 4 independent controllers.

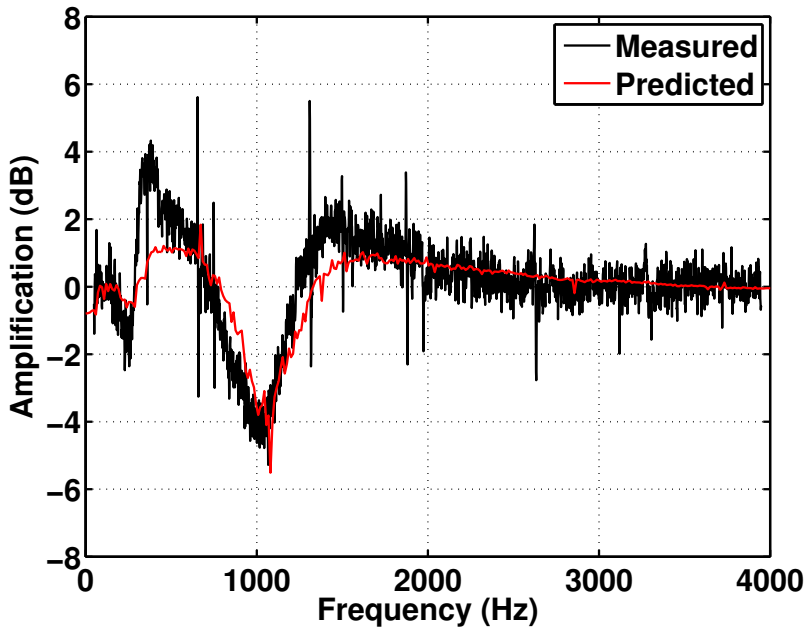

Figure 6.16 Comparison of predicted attenuation of sound power to measured attenuation in the far field.

Figure 6.17 is a three-dimensional representation of far-field noise attenuation at frequencies in the control band. The radius of the outer mesh represents the sound pressure level at every point on the hemisphere with control off. The inner mesh represents the sound pressure level with control on, and the level is designated by radius as well as color. This illustrates that, while the far-field attenuation is not perfectly uniform, the controller does not amplify the noise at any point on the hemisphere surrounding the fan.

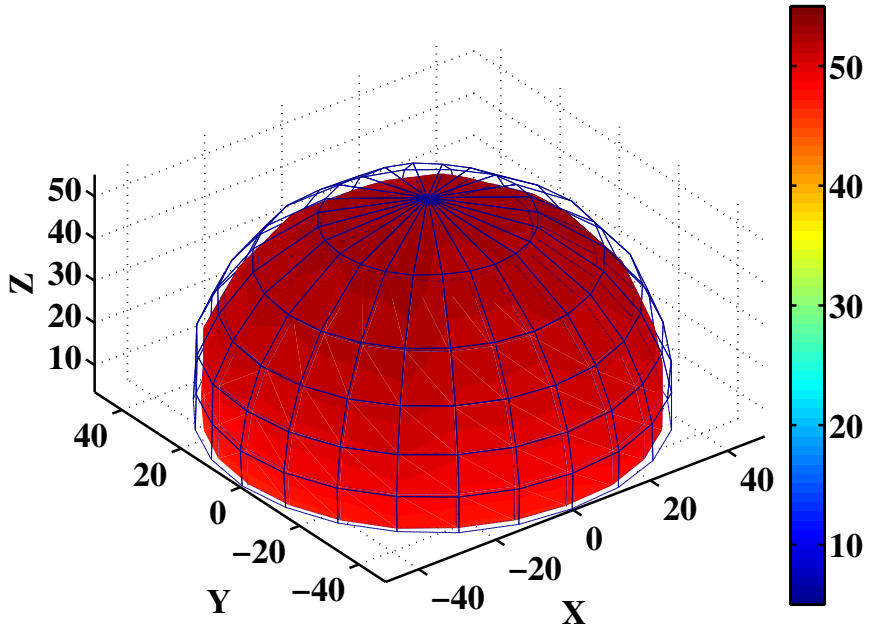

Figure 6.17 Balloon plot of far-field global control in the control band.

6.5 Hybrid control

The original goal of the current research was to develop a system that could be combined with the existing digital tonal controller to further attenuate fan noise. Therefore, it is not enough that the system perform well on its own. If the performance of the tonal controller is degraded by incorporating a feedback controller, this is not an acceptable outcome. Results are presented for both Filter #4 and Filter #5.

6.5.1 Filter #4

The broadband controller was incorporated in parallel with the tonal controller, with independent gain control between the two controllers. Figure 6.18 shows the near-field sound pressure at the error sensor without control, as well as with tonal and hybrid control. It is worth noting that the

amplification around the BPF of the fan is due to the tonal controller.

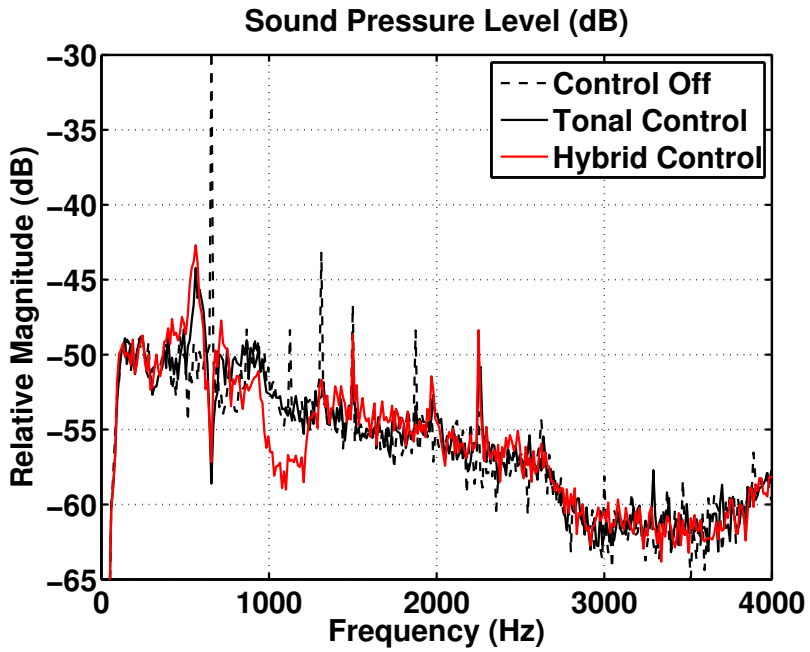

Figure 6.18 Near-field control performance using a hybrid tonal/broadband controller.

Figure 6.19 shows the far-field sound power of the fan with tonal control and with hybrid control, and Figure 6.20 demonstrates the increase in attenuation when incorporating the broadband controller. As with the broadband controller alone, the amplification outside the control band is greater in the far field than in the near field. Table 6.1 shows the amount of attenuation using the different controller configurations. The tonal controller alone offers over 2 dB of overall attenuation in the near field and the far field. However, due to the waterbed effect, the amplification out of band offsets the attenuation in band, and the broadband controller ends up amplifying the overall level of noise.

Filter #4	Near-Field Attenuation		Far-Field Attenuation	
Configuration	In-Band	Overall	In-Band	Overall
Broadband	1.9 dB	-1.3 dB	2.8 dB	-0.4 dB
Tonal	0.5 dB	2.9 dB	1.8 dB	2.6 dB
Hybrid	2.3 dB	2.2 dB	3.5 dB	1.7 dB

Table 6.1 Near-field and far-field control performance for all configurations using Filter #4

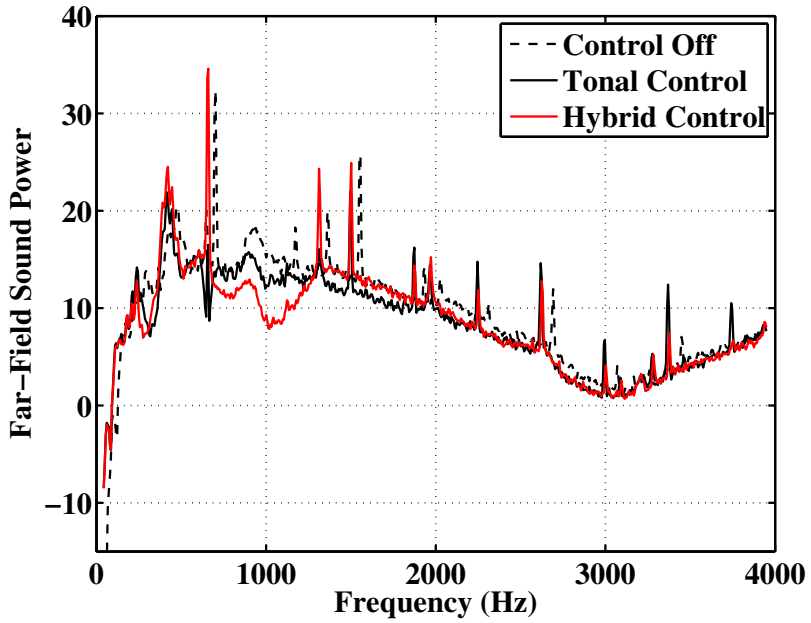

Figure 6.19 Far-field control performance using a hybrid tonal/broadband controller.

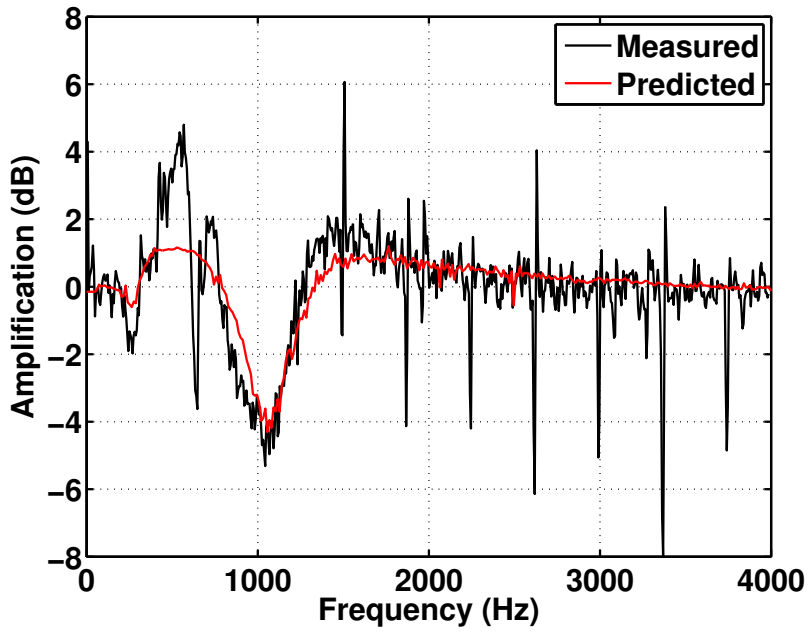

Figure 6.20 Comparison of predicted attenuation of sound power to measured attenuation in the far field.

6.5.2 Filter #5

Filter #5 was designed to attenuate noise below the BPF of the fan. This was partially due to the fact that the tonal controller amplifies the noise in this region, and the analog controller could potentially counteract this effect. Figure 6.21 shows that the controller is able to significantly reduce the noise in the region of control.

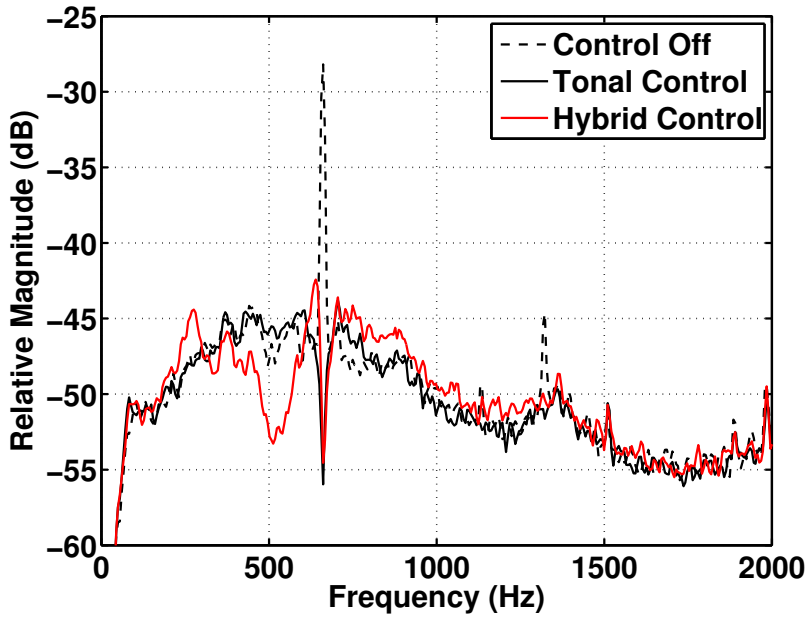

Figure 6.21 Near-field control performance using a hybrid tonal/broadband controller.

Figure 6.22 shows the far-field results using the tonal controller, as well as the hybrid controller. Figure 6.23 shows that the far-field attenuation corresponds well to prediction inside the region of control. Table 6.2 shows that this filter was able to attenuate the noise significantly in the region of control. However, the out-of-band amplification is increased in the far field. Unlike the previous controller, this filter provided a reduction in the overall level of the far-field noise, as seen below. However, the overall attenuation is small. Once again, the amplification out of band due to the waterbed effect almost entirely offsets the attenuation in the control band.

Filter #5	Near-Field Reduction		Far-Field Reduction	
Configuration	In-Band	Overall	In-Band	Overall
Broadband	2.2 dB	-0.1 dB	2.8 dB	0.1 dB
Tonal	1.8 dB	2.6 dB	-0.3 dB	0.3 dB
Hybrid	3.6 dB	2.5 dB	2.1 dB	0.4 dB

Table 6.2 Near-field and far-field control performance for all configurations using Filter #5

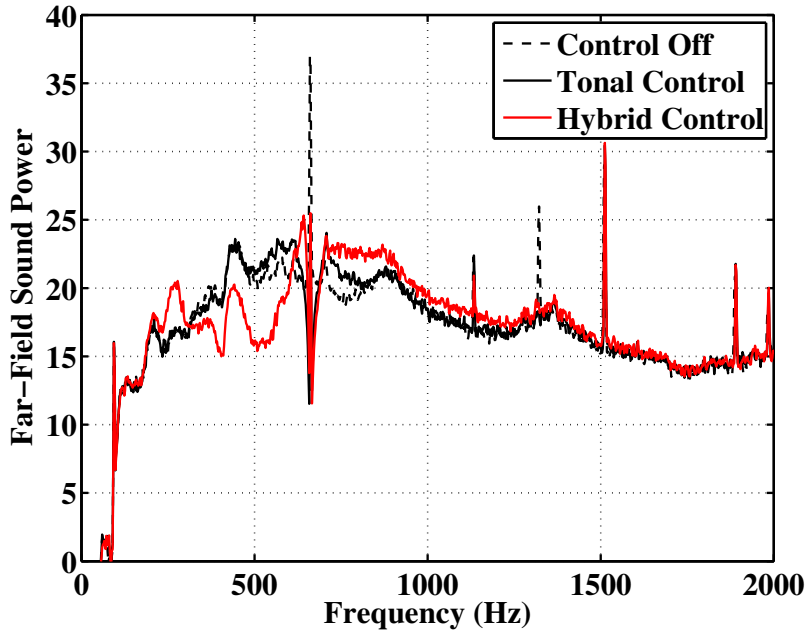

Figure 6.22 Far-field control performance using a hybrid tonal/broadband controller.

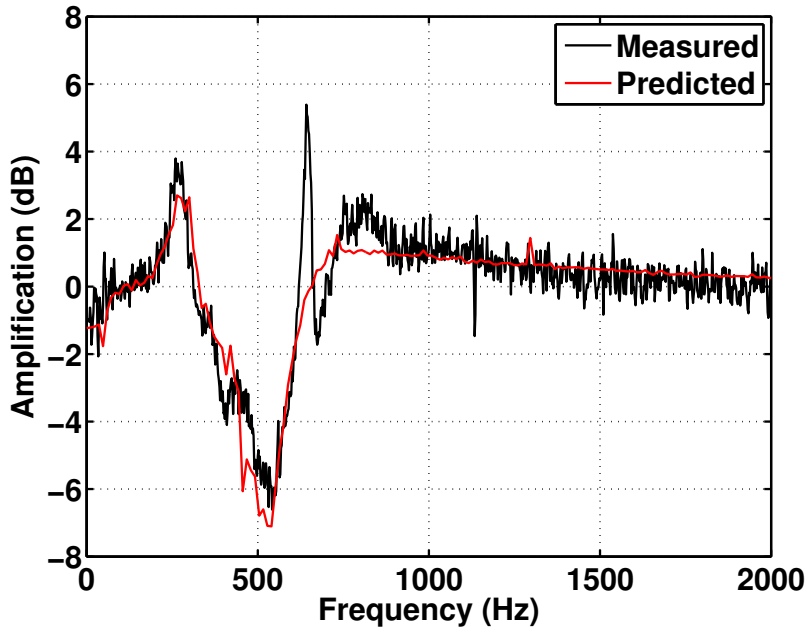

Figure 6.23 Comparison of predicted attenuation of sound power to measured attenuation in the far field.

Chapter 7

Conclusions and Recommendations for Future Work

The goal of the current research was to design a controller to attenuate broadband noise from an axial cooling fan. An analog feedback controller was chosen to overcome limitations imposed by the delay in digital systems. This system was then to be combined with an existing tonal noise controller to improve the overall effect of the system. A model was also developed for controller design and performance prediction.

It has been demonstrated that an analog feedback controller is a viable way of reducing broadband noise from an axial cooling fan. While broadband noise can be attenuated in some frequency range, this attenuation is achieved at the expense of amplifying noise outside of the frequency range of control. The range of frequency over which a controller can attenuate noise without amplifying the noise significantly outside the control range is dictated by the amount of delay in the plant.

It is suggested that this type of active control is ideal in situations where the plant has very little delay, such as an acoustic system with collocated error sensors and control actuators. Due to the band-limited nature of this type of control, it could also be used in situations where the disturbance

is not flat across frequency. For example, if the disturbance signal is generally non-deterministic, but is limited to a small frequency band, then the controller could be designed to attenuate noise in the region where the disturbance is greatest, and any amplification out of this band would be at lower levels.

It has also been shown that a feedback controller can be designed using a combination of well-known filter designs using simple topologies. Multiple types of control filters have been investigated, and their performance has been compared to a numerical model. The model accurately predicts the control performance at the error sensor near the fan. However, in the far field of the fan, the noise amplification below the control band is exaggerated. One possible explanation for this is that there may be evanescent energy in the near field of the fan that would typically decay before reaching the far field. When this noise is sensed at the error sensor, it is fed back to the loudspeakers, and is then converted to energy that propagates to the far field of the fan.

Future work should be done to investigate other types of control filter combinations. This thesis has outlined several control filters, and has shown the performance and limitations of each. It is possible that there are other types of filters that would offer a more favorable tradeoff between magnitude and phase, and would still be versatile enough to implement at different frequency ranges. Future work should also investigate the use of parallel control filters. Preliminary research was done to investigate the possibility of using parallel controllers to offset the waterbed effect of the primary controller. However, since the controllers were so close in frequency, they had detrimental effects on the primary controller. The use of parallel controllers spaced out in frequency should be investigated.

The analog feedback control system was implemented in parallel with an existing digital controller to further attenuate fan noise. It has been demonstrated that both systems perform as expected when the two are combined, and neither system has a detrimental effect on the other. This demonstrates that each controller can be designed independent of the other without needing to

account for the interaction of the two.

A model was used to predict the performance of a MIMO type controller. However, it was shown that the use of multiple SISO controllers is preferable for the current system. In every configuration that incorporated more than each loudspeaker and its nearest microphone, the control performance did not improve. This can be explained by the significantly reduced gain in the non-diagonal elements of the relative gain matrix. Therefore, the interactions of these channels is not significant enough to contribute to overall control, and the noise that any of these channels introduces outweighs the possible benefit from using a MIMO controller.

Bibliography

[1] P. Lueg, "Process of Silencing Sound Oscillations," US Patent 2,043,416 (1936).

[2] D. Guicking, "On the invention of active noise control by Paul Lueg," Journal of the Acoustical Society of America **87,** 2251–2254 (1990).

[3] J. Wang, L. Huang, and L. Cheng, "A study of active tonal noise control for a small axial flow fan," Journal of the Acoustical Society of America **117,** 734–743 (2005).

[4] K. L. Gee and S. D. Sommerfeldt, "Application of theoretical modeling to multichannel active control of cooling fan noise," Journal of the Acoustical Society of America **115,** 228–236 (2004).

[5] B. B. Monson, Master's thesis, Brigham Young University, 2006.

[6] M. J. Green, Master's thesis, Brigham Young University, 2006.

[7] B. M. Shafer, K. L. Gee, and S. D. Sommerfeldt, "Verification of a near-field error sensor placement method in active control of compact noise sources," Journal of the Acoustical Society of America **127,** EL66–EL72 (2010).

[8] A. V. Oppenheim and R. W. Schafer, *Discrete-Time Signal Processing*, 2 ed. (Prentice Hall, 1999).

[9] P. A. Nelson and S. J. Elliott, *Active Control of Sound* (Academic Press, 1992).

[10] S. Elliott, I. Stothers, and P. Nelson, "A multiple error LMS algorithm and its application to the active control of sound and vibration," Acoustics, Speech and Signal Processing, IEEE Transactions on **35,** 1423 – 1434 (1987).

[11] S. Elliott, *Signal Processing for Active Control* (Academic Press, 2001).

[12] S. Kuo, X. Kong, and W. Gan, "Applications of adaptive feedback active noise control system," Control Systems Technology, IEEE Transactions on **11,** 216 – 220 (2003).

[13] B. M. Shafer, Master's thesis, Brigham Young University, 2007.

[14] R. T. Stefani, *Design of feedback control systems* (Oxford University Press, New York, 2002).

[15] G. F. Franklin, *Feedback control of dynamic systems* (Pearson Prentice Hall, Upper Saddle River N.J., 2006).

[16] K. J. Astrom and R. M. Murray, *Feedback Systems* (Princeton University Press, 2008).

[17] S. Skogestad and I. Postlethwaite, *Multivariable Feedback Control* (John Wiley and Sons, 2005).

[18] E. Bristol, "On a new measure of interaction for multivariable process control," Automatic Control, IEEE Transactions on **11,** 133 – 134 (1966).

[19] S. Wang and N. Munro, "A complete proof of Bristol's relative gain array," Transactions of the Institute of Measurement and Control **4,** 53–56 (1982).

[20] R. P. Sallen and E. L. Key, "A Practical Method of Designing RC Active Filters," IRE Transactions on Circuit Theory **CT-2,** 74–85 (1955).

[21] D. J. Comer, *Continuous Time Filters: Passive, Active and Integrated*

[22] R. A. Pease, *Analog Circuits* (Newnes, 2008).

[23] P. Fleischer and J. Tow, "Design formulas for biquad active filters using three operational amplifiers," Proceedings of the IEEE **61,** 662 – 663 (1973).

[24] K. L. Su, *Analog filters* (Kluwer Academic Publishers, Norwell, 2002).

[25] J. D. Sagers, T. W. Leishman, and J. D. Blotter, "Active sound transmission control of a double-panel module using decoupled analog feedback control: Experimental results," Journal of the Acoustical Society of America **128,** 2807–2816 (2010).

[26] T. Deliyannis, "High-Q factor circuit with reduced sensitivity," Electronics Letters **4,** 577 –579 (1968).